Numerical Analysis of Residential Electricity Generation Using Solar Thermal Energy

Undergraduate Honors Thesis

Presented in Partial Fulfillment of the Requirements for

Graduation with Distinction

at The Ohio State University

By

Jake Wither

* * * * *

The Ohio State University

2010

Defense Committee:

Yann Guezennec, Advisor

Marcello Canova

Approved by

_____

Adviser

Undergraduate Program in Mechanical Engineering

Abstract

Currently, the world has an ever increasing energy demand and available resources such as fossil fuels are not a sustainable option for the future. Solar thermal electricity generation is one option to curve this problem, but the technology is currently limited to large utility scale. This thesis explores the fluid selection process and optimization of an Organic Rankine Cycle that could provide the electrical load of a residential home. Four working fluids (R600a/iso-butane, n-pentane, methanol and ethanol) and four system configurations (Rankine with and without superheating, open loop and closed loop pre-heating) were parametrically explored to see if it was feasible to create a system with efficiencies that were competitive with current photovoltaic technology. The results found that for low grade solar heat in the range of 80-125° C, the best system (efficiency up to 14%) consisted of a regular four stage Rankine cycle with iso-butane as the working fluid. If input temperature of 100-150° C can be reached, a closed loop pre-heater design with n-Pentane can produce very effective systems (15-21%). Methanol and ethanol seem best suited for higher temperature applications were the possibility of co-generation could be explored. Residential solar thermal electricity generation is a feasibly technology and as solar collects and micro expanders develop more, it can become a leader in renewable energy.

Acknowledgements

I would like to thank the other members of the research team Mike Nesteroff, Brad Engel, and Nick Warner for helping to explore this topic with me. Thank you to F-Chart Software which developed Engineering Equation Solver, which made the analysis of this thesis possible. A special thanks to my advisor Dr. Yann Guezennec for helping to coordinate this project.

Table of Contents

List of Figures

List of Tables

Chapter 1: Introduction and Overview

1.1 Introduction

Human beings consume and demand more energy every day. Up until recent years, mother earth has satiated our ever growing thirst in a way that seemed as though her resources would never expire. Non-renewable energy sources like coal and petroleum were so bountiful that they were used without fear of depletion. The reality is starting to set in that these energy sources, which have been inside the earth for so long they have earned the name fossil fuels, are finite. This knowledge is also coupled with the fact that these fuels are having detrimental effects on our planet's delicate ecosystem. The combustion as well as the extraction of these energy sources is altering our environment in ways that may never be fully understood. Within the matter of weeks, oil spills like the BP disaster in the Gulf of Mexico as well as mountain top removal processes to cheaply mine coal can completely alter ecosystems that have taken enormous amount of time to develop. Then when needs like transportation or electricity demand the burning of these fuels, harmful gases like carbon dioxide, sulfur oxides, and nitrogen oxides are released into the atmosphere.

To help curve our dependence on these fossil fuels, researchers and scientist have been exploring renewable energy sources that are both environmentally friendly and sustainable. These renewable energy sources include: wind energy, modern biomass, geothermal energy, hydropower, and solar energy. Unfortunately, many of these have technological drawbacks or are not economically competitive with fossil fuels. This is why as of 2008, only two percent of the world's total energy demand was supplied by one of the mentioned options [1].

The kinetic energy of the wind can be captured and transformed into electricity by coupling wind turbines with a generator. This technology has zero emissions and currently

accounts for 0.3% of the installed electricity generation globally. However due to the inconsistency of the wind, on average these turbines only supply 0.1% of the total global energy [2]. The main drawback of wind energy is that the construction of wind farms can create an eyesore for the surrounding areas and the presence of these large windmills can disrupt the migratory patterns of birds. Another disadvantage to harnessing wind power is that some of the sites best suited for the technology are remote and disconnected from the communities and areas that need the electricity. This separation between the production and end use of the electricity causes higher costs associated with transmitting the power [3].

In under developed areas like Africa, Asia and Latin America, wood, the simplest form of biomass, is a primary source for heat and cooking [1]. New forms of modern biomass such as ethanol are starting to be used to generate electricity and fuel transportation. The advantages of this energy source are that the process of turning living matter into a fuel is rather basic and there are not many limitations on where the technology can be implemented. However, like wind power, there are problems facing biomass. The systems involve large land and water requirements as well as increased fertilizers and herbicide usage [3].

There is a vast amount of energy below the surface of the earth that can be captured and utilized via geothermal power. According to scientists, there is enough untapped energy in the earth's crust to supply the United States with power for the next 30,000 years [3]. Unfortunately, the technology and research in the field of geothermal power is still rather underdeveloped in terms of its potential. Besides being underdeveloped, geothermal wells have the potential to release harmful gases such as sulfur into the atmosphere. Today the main use of geothermal energy is for residential heating and this application is quickly growing. Electricity generation from geothermal has so far been limited to a few demonstration sites around the world.

Hydroelectric power uses the elevation change in rivers to turn turbines and generate electricity. This form of renewable energy very minimal emissions throughout its life cycle and can be built rather inexpensively with respect to other sustainable technologies. Although hydroelectric benefits the environment by limiting harmful gases that are associated with burning fossil fuels, the implementation of this technology damages ecosystems. When a dam is constructed or a river rerouted, the natural habits that have take thousands of years to develop are completely altered. This sudden change can destroy the equilibrium of the natural system and the wildlife that depend on it. Hydroelectric is, however, the oldest and most developed renewable energy source for electricity. It accounts for 7% of the United States total electrical load and around 56% of the electrical needs in Switzerland. The problem is that most rivers that can be economically dammed have already been and it is unlikely that significant future growth is possible.

The final source of renewable energy, which is the both the most abundant as well as the topic of discussion for this paper, is solar energy. There are two ways to harness the energy from the sun to produce electricity. The first and most common way to do this is through photovoltaic (PV) panels. PV panels are made of a silicon based semiconductors which absorb the energy from the sun and turn it directly into electricity. The second way to turn sunlight into electricity is an indirect conversion which takes the heat energy of the sun and uses it as the input to a power generation cycle such as a Rankine cycle, which will be discussed in detail in the methodology section. Table 1 on the next page shows a breakdown of the differences between photovoltaic and solar thermal electricity generation and why the latter is a better technology. The table shows that the price of electricity generation on the utility scale is currently cheaper for

Table 1: Comparison of Solar Energy Technology

	Photovoltaic Cells	Solar Thermal
Average Cost of Electricity (2005)[3]	18-31 Cents/kWh	11-15 Cents/kWh
Energy Storage	Electrical	Electrical and Thermal
Co-Generation Capabilities	N/A	Hot Water Tank Heating Space Heating
CO_2 Emission[1]	98-167 g/kWh	26-38 g/kWh
NO_x Emission[1]	0.18-0.3 g/kWh	0.06-0.13 g/kWh

solar thermal applications. While both systems have the capability of electrical energy storage, the solar thermal system can also store heat collected from the sun which is more effective and cheaper than battery storage. Co-generation, which is the utilization of energy for processes other than electricity generation, is a quality that is not available in PV panels. When the entire life cycle of the two technologies is compared, solar thermal systems will emit less CO_2 and NO_x for every kWh they produce. For the reasons mentioned above, solar thermal electricity generation has been chosen as the renewable energy to be explored in depth by this thesis.

1.2 Motivation

Currently the majority of solar thermal electricity generation is done on the utility scale and there has been very little research dedicated to technology with smaller power outputs. This lack of investigation is partially due to hardware constraints which have made the down scaling of the technology unpractical until recent years. Advancements in solar collector devices as well as small scale expanders have opened the door to explore new types of configurations. There are many benefits that can be achieved if solar thermal systems can be scaled down efficiently. The technology could be used to give electricity to rural or remote areas were electrical lines are too

costly to implement. The system could be used for military applications as well as car charging stations to meet the demand of electric vehicles that will be populating future roads. The main advantage of a small scale solar thermal system would be electricity generation for residential homes. Along with giving the user energy independence from a clean and renewable source; the residential design will allow for the utilization of excess energy for procedures like space heating in the winter as well as hot water generation.

1.3 Literature Review

While there are not many small scale solar thermal systems in operation, there has been research done looking at low-grade heat-driven Rankine cycles. One of the starting points for the background research on this project (albeit, in a different field) was another OSU undergraduate's honors thesis. Under the supervision of Dr. Yann Guezennec, Leon Headings [4] explored the possibility of a low grade heat electricity generation system for automotive applications. Using waste heat recovery with an organic Rankine cycle, Headings investigated four working fluids, R113, R123, R134a, and steam with the heat input coming from a car's radiator and/or exhaust system. The results showed that R134a was best suited for the low grade heat and could achieve an 8.5% system efficiency with a power output of 1.5 kW [4].

Along with that paper, there have been several other studies that looked at either actual prototypes of small scale solar thermal applications or theoretical investigations of these systems. One paper documented a design and implementation of a prototype Rankine cycle that used n-pentane as the working fluid. The system used water heated by a gas fired boiler to raise the working fluid to a temperature of 81° C at the inlet of the expander, with a pressure of 4 Bar. Theoretically, it was predicted that the system should be able to produce 1.5 kW of electricity

with a thermal efficiency of 10.6% when the condensing temperature was 38° C. However, when the experiments were run, the actual efficiency of the system ended up only being 4.3% [5]. Figure 1 on the next page shows a comparison of thermodynamic efficiency of seven possible working fluids over a range of expander inlet temperatures. The efficiencies were solved for a four stage Rankine cycle with a pump efficiency of 85%, expander efficiency of 75%, and pressure ratio of 3 which is typical of scroll expanders [6].

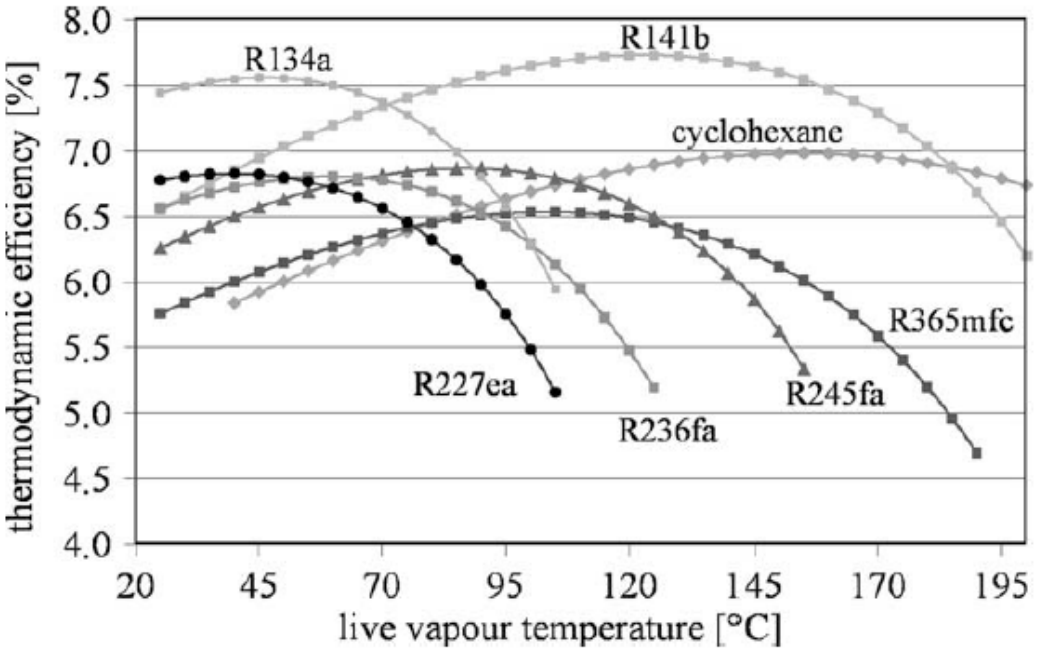

Figure 1: Efficiency of Varying Fluids [6]

Table 2 shows the results of Rankine cycles with (+) and without (-) internal heat exchangers (IHE) for ten different working fluids. All of the substances received the same amount of input energy, resulting in a desired exit temperature of 145° C, and they were completely saturated at the expander inlet. The table gives data for expander inlet pressure (p_{max}) and temperature (t_3), expander outlet pressure (p_{min}) and temperature (t_4), mass flow rate (m), net work of the system (W_n), thermal efficiency (η_{thm}) and many others [7]. These outputs help to better understanding of what types of efficiencies and other parameters are to be expected out of low grade heat Rankine cycles.

Table 2: Output of Rankine Cycle With and Without Pre-Heater for Various Working Fluids [7]

Substance	Unit	Ammonia		Butane		Isobutane		R11	R123		R141B		R236EA		R245CA		R113		Water
Type		A		C		C		C	C		C		C		C		C		A
IHE		−IHE	+IHE	−IHE	+IHE	−IHE	+IHE	−IHE	−IHE	+IHE	−IHE	+IHE	−IHE	+IHE	−IHE	+IHE	−IHE	+IHE	−IHE
t_c	°C	132.25	132.25	152.01	152.01	134.70	134.70	197.96	183.68	183.68	204.20	204.20	139.29	139.29	174.42	174.42	214.06	214.06	373.99
p_c	MPa	11.333	11.333	3.796	3.796	3.640	3.640	4.408	3.662	3.662	4.25	4.25	3.502	3.502	3.925	3.925	3.392	3.392	22.064
t_{in}	°C	145.0	145.0	145.0	145.0	145.0	145.0	145.0	145.0	145.0	145.0	145.0	145.0	145.0	145.0	145.0	145.0	145.0	145.0
Δt	°C	8.0	8.0	8.0	8.0	8.0	8.0	8.0	8.0	8.0	8.0	8.0	8.0	8.0	8.0	8.0	8.0	8.0	8.0
t_{out}	°C	71.15	72.04	64.53	67.90	60.45	63.91	71.77	68.10	70.25	70.49	71.20	59.59	65.45	66.22	70.08	68.81	72.99	79.07
t_3	°C	135.00	135.00	85.54	85.54	87.15	87.15	82.09	83.23	83.23	81.72	81.72	87.73	87.73	85.17	85.17	83.44	83.44	135.00
t_4	°C	37.01	37.01	40.84	40.84	40.10	40.10	29.26	38.44	38.44	33.5	33.5	45.42	45.42	43.10	43.10	45.38	45.38	25.00
$t_{in,evp}$	°C	26.43	29.85	25.81	33.25	26.20	32.84	25.39	25.35	30.91	25.29	27.47	25.74	36.33	25.36	34.36	25.19	36.23	25.01
p_{min}	MPa	1.003	1.003	0.244	0.244	0.350	0.350	0.106	0.091	0.091	0.079	0.079	0.206	0.206	0.101	0.101	0.045	0.045	0.003
p_{max}	MPa	3.90	3.90	1.14	1.14	1.55	1.55	0.55	0.53	0.53	0.44	0.44	1.20	1.20	0.65	0.65	0.29	0.29	0.046
x	/	1	1	1	1	1	1	1	1	1	1	1	1	1	1	1	1	1	0.95
v_4	m^3/kg	0.137	0.137	0.173	0.173	0.118	0.118	0.166	0.179	0.179	0.270	0.270	0.080	0.080	0.188	0.188	0.310	0.310	41.23
m	kg/s	0.93	0.93	3.14	3.14	3.61	3.61	6.06	6.47	6.47	4.86	4.86	7.47	7.47	5.49	5.49	7.02	7.02	0.43
W_{TBN}	kW	161.60	161.60	170.34	170.34	180.91	180.91	154.38	160.14	160.14	155.17	155.17	178.34	178.34	164.53	164.53	157.61	157.61	139.67
W_{PUMP}	kW	7.45	7.45	8.18	8.18	13.07	13.07	3.04	3.23	3.23	2.37	2.37	8.68	8.68	3.62	3.62	1.84	1.84	0.03
W_n	kW	154.15	154.15	162.16	162.12	167.84	167.84	151.34	156.91	156.91	152.80	152.80	169.66	169.66	160.90	160.90	155.77	155.77	139.64
Q	kJ/s	1274.08	1258.84	1387.23	1329.58	1456.85	1397.71	1263.49	1326.13	1289.34	1285.38	1273.11	1471.47	1371.45	1358.33	1292.24	1313.98	1242.47	1138.46
I_{EVP}	kJ/s	152.79	150.06	162.57	153.20	164.86	155.82	156.54	161.25	154.85	159.35	157.10	166.03	151.13	161.27	150.30	159.95	147.81	146.95
I_{TBN}	kJ/s	27.42	27.42	28.30	28.30	30.11	30.11	26.68	26.86	26.86	26.49	26.49	29.17	29.17	27.15	27.15	25.84	25.84	24.23
I_{CND}	kJ/s	19.15	18.72	22.84	19.89	24.03	21.04	18.76	20.92	19.20	19.44	18.96	26.32	20.52	22.78	19.21	22.51	18.43	16.78
I_{PUMP}	kJ/s	2.92	2.92	3.21	3.21	5.13	5.13	1.19	1.27	1.27	0.93	0.93	3.41	3.41	1.42	1.42	0.72	0.72	0.01
I_{IHE}	kJ/s	/	0.29	/	1.14	/	1.14	/	/	0.73	/	0.22	/	2.17	/	1.41	/	1.57	/
E_{out}	kJ/s	122.10	125.24	99.71	110.90	86.83	97.73	124.28	111.58	118.98	119.78	122.29	84.21	102.73	105.26	118.39	114.00	128.66	151.18
η_{thm}	%	12.10	12.25	11.69	12.20	11.52	12.01	11.98	11.83	12.17	11.89	12.00	11.53	12.37	11.85	12.45	11.85	12.54	12.27
η_{exg}	%	32.20	32.20	32.87	33.87	35.05	35.05	31.61	32.77	32.77	31.91	31.91	35.43	35.43	33.61	33.61	32.53	32.53	29.17

As mentioned earlier, the hardware of these small scale solar thermal systems play a very significant role determining the efficiency and even feasibility of power generation. The solar collectors determine how much energy is brought into the system. Depending on the type of collector selected, there is a wide range of expander inlet temperatures that can be reached. On the low end, static solar collectors that don't have any source of concentration can produce temperatures of around 80° C. The next level up is known as low concentration solar collects, and this category includes compound parabolic concentrators or systems that involve Fresnel lens. These collectors can reach anywhere from 100-150° C. The most complex collectors on the market are parabolic troughs which can reach from 200-250° C [8]. While the collector determines the heat input of the cycle, the expander plays a major role in the cost of the overall system. A feasibility study was done to explore the practicality of a low grade heat Rankine cycle, and it was found that nearly half of the entire system was the expander [9].

1.4 Project Objectives

In order to further explore the possiblity of solar thermal electricity generation on the residential scale, a research team of three OSU undergraduate honors students was assembled under the supervision Dr. Yann Guezennec. Michael Nesteroff researched available solar collector technology to find the one that best meets our project needs. Brad Engel was in charge of exploring a small expander device that will be the output of the Rankine cycle. This thesis was to choose possible working fluids to investigate in depth. Once the substances have been decided on, a parametric study of system inlet conditions as well as system configurations will be preformed to try and bracket the possible system efficiencies.

Chapter 2: Methodology

2.1 Rankine Cycle

Michael Moran and Howard Shapiro discuss several power generation cycles in *Fundamentals of Engineering Thermodynamics* [10]. Of these designs, the four stage Rankine cycle is the most basic and common. Figure 2 below shows the hardware for the system layout of the cycle on the left and a thermodynamic schematic on the right. The graph is known as a T-s diagram, which shows the relationship between temperature and entropy, usable energy, when a substance goes through a phase change from liquid to gas. The curve is known as the vapor dome, and any point on the left of the dome represents a substance that is completely in the liquid state, and alternatively any point that is on the left of the vapor dome is one hundred percent in the gaseous phase. Inside the vapor dome, substances are in a transitional state and are a combination of liquid and gas. The lines that points one and four are on as well are two and three are on, are constant pressure lines with the latter being the more pressurized of the two.

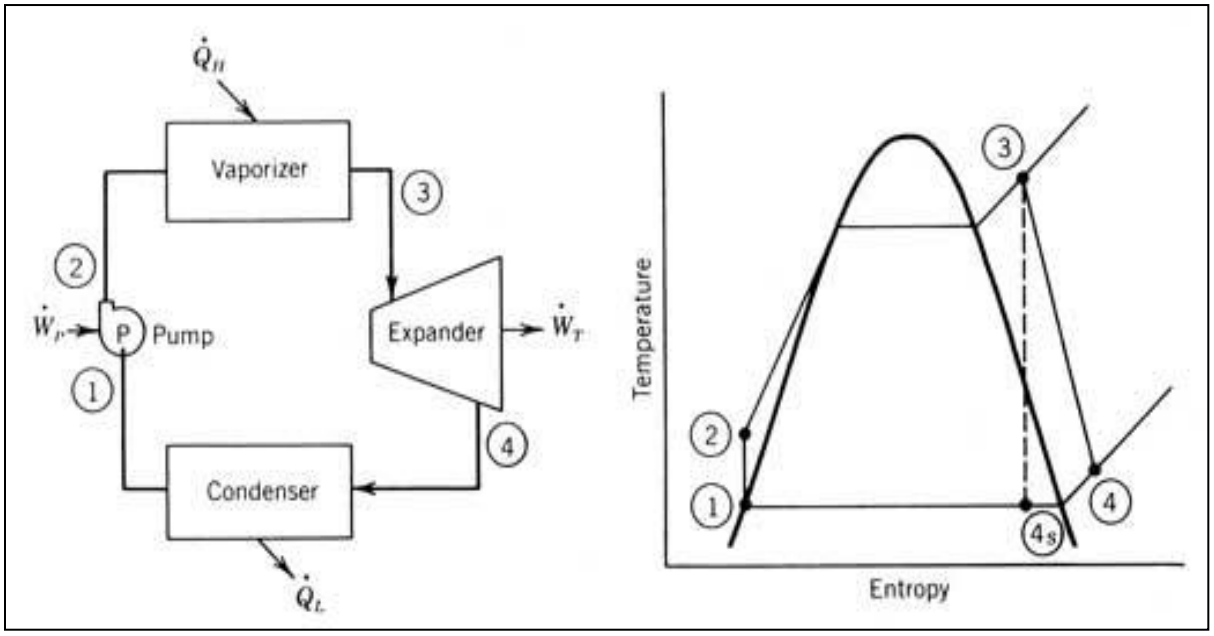

Figure 2: System Configuration and Temperature-Entropy Diagram of Ordinary Rankine Cycle

As Figure 2 shows, the four hardware components of the design are the vaporizer (or boiler), expander (or turbine), condenser, and pump. The closed loop cycle works as follows; at point one the working fluid is completely in the liquid state and at a low pressure. The pump is used to (ideally, isentropically) raise the pressure of the working fluid. The pressurized liquid coming out of the pump at point two is then heated by the vaporizer until it is fully evaporated and possibly superheated. Next, the high pressure gas is run through an expander which will output usable work and yield a low pressure gas or high temperature liquid/gas mixture. In order to get the substance back to a fluid which can be run through the pump, the condenser rejects heat until cycle is back at state one. For this thesis, certain assumptions about the Rankine cycle were made. It was assumed that both the vaporizer and condenser operate at constant pressures and the efficiencies of the pump and expander were 80%.

Being that the Rankine cycle is the simplest thermodynamic cycle for power generation, it was decided to be the first area of exploration for the research project. By knowing the state properties at the different stages of the cycle, different thermodynamic qualities of the cycle can be determined. Figure 3 shows the basic equations for evaluating a Rankine cycle.

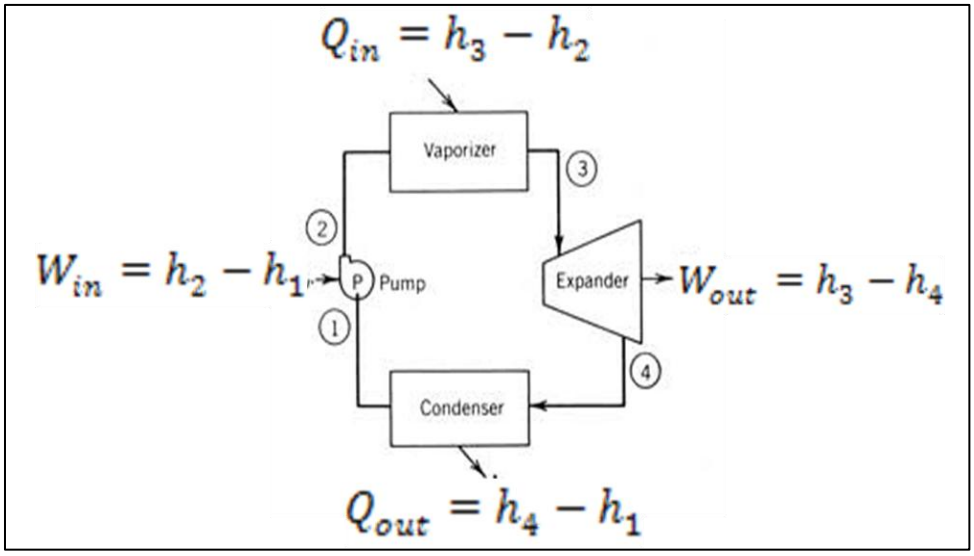

Figure 3: System Equations for Regular Rankine Cycle

The amount of Q_{in}, or energy added to the system, can be found by calculating the enthalpy at state two and subtracting it from the enthalpy at state three (h_3-h_2). It should be noted that the value of Q_{in} will be dependent on flow rate and will be in terms of energy transferred per unit mass. The amount of work per unit mass produced by the expander can be calculated by finding the difference in enthalpy from state three to state four. Likewise, the amount of work put into the pump can be found by the subtraction of the enthalpy at one from the enthalpy at state two.

$$W_{net} = W_{out} - W_{in} \qquad (1)$$

$$System\ Efficiency = \eta = \frac{W_{net}}{Q_{in}} \qquad (2)$$

Equations (1) and (2) show how to calculate the net work of the system (work produced by the expander minus the work put into the pump) as well as the overall efficiency of the cycle (dividing the net work by the energy put into the cycle). A more in depth look into solving for system parameters will be covered in Section 2.3 about the Engineering Equations Solver.

2.2 Working Fluid Selection Process

The majority of Rankine power generation cycles currently use steam as the working fluid in system. Water is normally utilized because it is the most abundant fluid on the Earth, it has a relatively low boiling temperature under reasonable pressures, and it is very cheap. Typical operation conditions for water vapor power generation Rankine cycles include temperatures ranging from 360° C to 540° C (superheating) at a pressure of around 190 bar. Since for this research project the energy input for the vaporizer is going to from a low grade solar thermal collector, a working fluid other than water will be more suitable to the design. Performance parameters, environmental concerns, and other consideration were taken into account during the

selection process. This section of the thesis discusses the narrowing down and selecting of four working fluids to be parametrically explored in depth.

The first constraint that was considered when searching for possible working fluids was operating parameters such as temperature and pressure on both the low and high ends. All of these requirements were functions of the hardware capabilities of the power generation system. As discussed in Section 2.1, in order for a Rankine cycle to complete, the fluid has to be able to go through a phase change from liquid to gas and then back to a liquid. In order to properly design a system, these phase changes need to occur at temperatures and pressures that are achievable by the collectors and scroll expander. From the literature review, it was found that the extremes of current solar collector capacities range from 80 ° C to 200 ° C for flat plate and parabolic trough collectors respectably. Figure 4 gives a graphical representation of the possible range that selected substances need to have a phase change from liquid to gas on the high side as well as the range that condensation must occur at on the low temperature side. As mentioned, the high side is dictated by the solar collectors' capabilities, while the cold side is dependent on how energy will be rejected from the system. The high end of 40 ° C corresponds to the fluid being condensed using a heat exchanger with summer time air as the heat sink and the 15° C represents a heat sink of ground water.

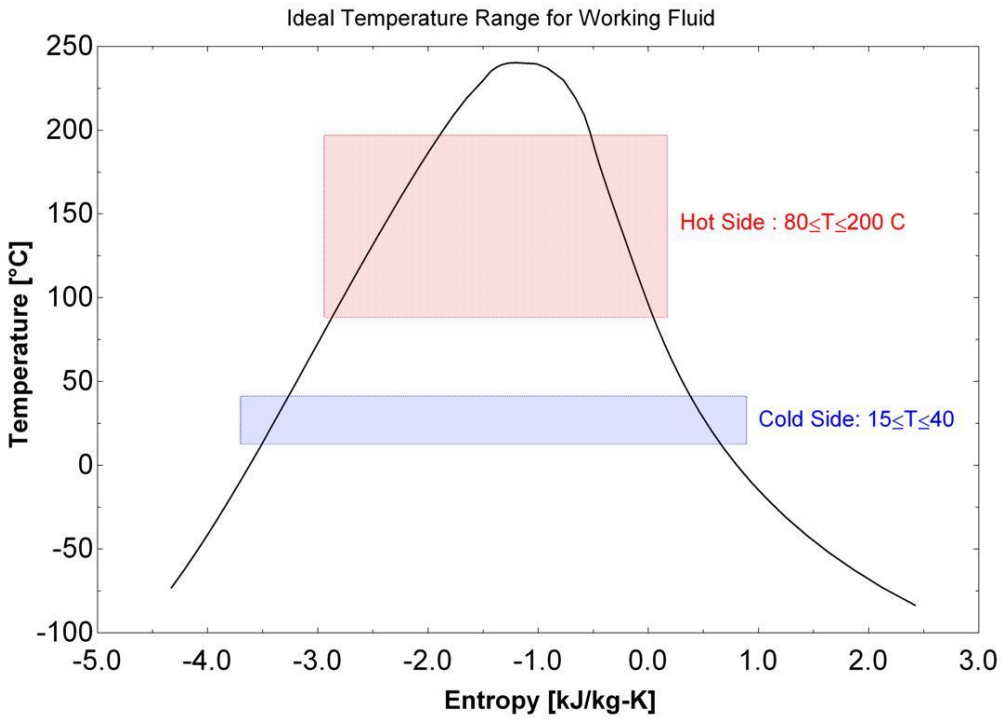

Figure 4: Ideal Temperature Range for Working Fluid

Along with these temperature constraints, there are pressure attributes that the selected fluids must contain. Due to limitations of the micro scroll expander that Brad Engel is exploring, the phase change from liquid to gas needs to occur in a pressure range of 5 to 20 Bar. The critical pressure of the fluid, which is the peak of the vapor dome, must be at least 25 Bar.

While finding a working fluid that fits best within the constraints of the hardware of the system was the primary factor in the selection process, environmental concerns came in at a very close second. When looking at possible candidates there were three main environmental concerns that were considered: Ozone Depletion Potential (ODP), Global Warming Potential (GWP), and atmospheric lifetime.

Table 3: Physical, Safety, and Environmental Data of Working Fluids [11]

Physical, safety and environmental data of the working fluids.

Substance		Physical data				Safety data	Environmental data		
		Molecular mass (kg/kmol)	T_{bp}[a] (°C)	T_{crit}[b] (°C)	P_{crit}[c] (MPa)	ASHRAE 34 safety group	Atmospheric life time (yr)	ODP[d]	GWP[e] (100 yr)
1	RC318	200.03	−6.0	115.2	2.778	A1	3200	0	10,250
2	R600a	58.12	−11.7	135	3.647	A3	0.019	0	~20
3	R114	170.92	3.6	145.7	3.289	A1	300	1.000	10,040
4	R600	58.12	−0.5	152	3.796	A3	0.018	0	~20
5	R601	72.15	36.1	196.5	3.364	–	0.01	0	~20
6	R113	187.38	47.6	214.1	3.439	A1	85	1.000	6130
7	Cyclohexane	84.16	80.7	280.5	4.075	A3	n.a.	n.a.	n.a.
8	R290	44.10	−42.1	96.68	4.247	A3	0.041	0	~20
9	R407C	86.20	−43.6	86.79	4.597	A1	n.a.	0	1800
10	R32	52.02	−51.7	78.11	5.784	A2	4.9	0	675
11	R500	99.30	−33.6	105.5	4.455	A1	n.a.	0.738	8100
12	R152a	66.05	−24.0	113.3	4.520	A2	1.4	0	124
13	R717 (ammonia)	17.03	−33.3	132.3	11.333	B2	0.01	0	<1
14	Ethanol	46.07	78.4	240.8	6.148	n.a.	n.a.	n.a.	n.a.
15	Methanol	32.04	64.4	240.2	8.104	n.a.	n.a.	n.a.	n.a.
16	R718 (water)	10.2	100	374	22.064	A1	n.a.	0	<1
17	R134a	102.03	−26.1	101	4.059	A1	14.0	0	1430
18	R12	120.91	−29.8	112	4.114	A1	100	1.000	10,890
19	R123	152.93	27.8	183.7	3.668	B1	1.3	0.020	77
20	R141b	116.95	32.0	204.2	4.249	n.a.	9.3	0.120	725

n.a., non-available.
[a] T_{bp}: normal boiling point.
[b] T_{crit}: critical temperature.
[c] P_{crit}: critical pressure.
[d] ODP: ozone depletion potential, relative to R11.
[e] GWP: global warming potential, relative to CO_2.

Table 3 lists environmental data for twenty different substances. Both the ODP and GWP of the substances are determined by comparing them to ODP and GWP of the refrigerant R11 and CO_2 respectably. The table also shows safety concerns with different working fluids. Since the system will be in close proximity of residential homes concern about possible leaks and explosions were considered. Extra caution will might need to be put into the housing of the power generation cycle in order to prevent harmful dangers.

As listed in Table 4, there were four different fluids that meet the hardware constraints as well as environmental concerns. Once possible working fluids meet the requirements of

Table 4: Working Fluids that Meet Performance and Environmental Properties

Fluid	Evaporation Temperature At 20 Bar	Evaporation Temperature At 15 Bar	Condensation Temperature At 5 Bar	Condensation Temperature At 1 Bar	Critical Temperature	Critical Pressure (Bar)	ODP	GWP
R600a	101.1 C	86.3 C	37.87 C	-12.18 C	135 C	36.47	0	20
n-Pentane	163.3 C	146.7 C	92.74 C	35.49 C	196.5 C	33.64	0	11
Methanol	166.4 C	153.8 C	111.9 C	64.67 C	240.2 C	81.04	n.a.	n.a.
Ethanol	180.8 C	167.7 C	125.2 C	77.94 C	240.8 C	61.48	n.a.	n.a.

performance parameters as well as environmental concerns, there were only two other requirements that needed to be fulfilled. In order for the substance to be used in a residential solar thermal electricity generation configuration, it must be available commercially at a reasonable price. The final qualification has nothing to do with system parameters or real world constraints, but rather it depends on whether or not it can be thoroughly explored using the Engineering Equations Solver (EES) software.

2.3 Introduction to Engineering Equation Solver (EES)

Engineering Equation Solver is a thermodynamic based software developed by Dr. William Beckman and Dr. Sanford Klein of the University of Wisconsin and is academically and commercially available from F-Chart Software. The program has built in tables of thermodynamic properties (entropy, enthalpy, temperature, pressure etc.) for over a hundred different substances and can simultaneously solve multiple sets of equations. The software can be programmed to explore a cycle system efficiency, net work, and/or power output. EES can

also be used to optimize certain qualities of a cycle. Figure 5 is a sample EES code for a regular Rankine cycle with R600a as the working fluid. Using properties like temperature and quality, EES will solve for enthalpy. The enthalpy at the different states can be used to solve for quantities like net work and system efficiency as shown under the System Equations section.

```
{R600a Pinned on Vapor Dome}

{Parameters}
eta_t=0.8
eta_p=0.8
{State 1}
x1=1
p1=pressure(R600a,T=T1,x=x1)
s1=entropy(R600a,T=T1,x=x1)
h1=enthalpy(R600a,T=T1,x=x1)
{State 2s}
s2s=s1
T2s=temperature(R600a,p=p2s,s=s2s)
h2s=enthalpy(R600a,T=T2s,s=s2s)
{State 2}
eta_t=(h1-h2)/(h1-h2s)
p2=p2s
{State 3}
p3=p2
x3=0
T3=25
s3=entropy(R600a,p=p3,x=x3)
h3=enthalpy(R600a,p=p3,x=x3)
p3=pressure(R600a,T=T3,x=x3)
{State 4s}
s4s=s3
p4s=p1
h4s=enthalpy(R600a,p=p4s,s=s4s)
{State 4}
eta_p=(h4s-h3)/(h4-h3)
{System Equations}
Wt_dot=(h1-h2)
Wp_dot=(h4-h3)
Qin_dot=(h1-h4)
Qout_dot=(h2-h3)
W_net=Wt_dot-Wp_dot
eta=W_net/Qin_dot
p_rat=p1/p2s
```

Figure 5: Sample EES Code for Rankine Cycle

2.4 ORC Parameters of Interest for Simple Rankine Cycle

There were four system inputs that were explored when using EES. Table 5 below depicts all the parameters that were bracketed when exploring the possibility of different working fluids. By allowing the values to vary over a large range, the capability of the power generation cycle can be found. As mentioned in section 2.2, the high side temperature of the cycle will be determined by the performance of the solar collectors. The expander design will be the limiting factor for both the high and low pressures in the cycles. The condenser temperature will depend on where the excess heat of the system is going to be rejected to.

Table 5: Governing Factors for Parametric Study

Parameter to be Explored	Minimum Value	Maximum Value	Governing Element
Expander Inlet Temperature (C)	80	200	Solar Collectors
Expander Inlet Pressure (Bar)	5	20	Expander Design
Expander Pressure Ratio	2	15	Expander Design
Bottom Condenser Temperature (C)	15	40	Ambient Temperature Source

2.5 Exploration of Alternative System Configuration

The simple four stage Rankine cycle is not always the best choice for a power generation cycle. Modifications to the simple Rankine cycle will add complication to the hardware but it can also potentially boost the efficiency of the system. All of the different system options that were looked at operate on the same basic principles as the ORC. Three other configurations similar to enhancements commonly used for steam Rankine cycle were explored: Superheating, Open-Loop Pre-Heating (open feed-water), and Closed-Loop Pre-Heating (closed feed-water) [10].

2.5.1 Super Heating

The most basic adjustment that can be made to a Rankine cycle comes in the form of superheating. This process requires no additional hardware, only additional energy input.

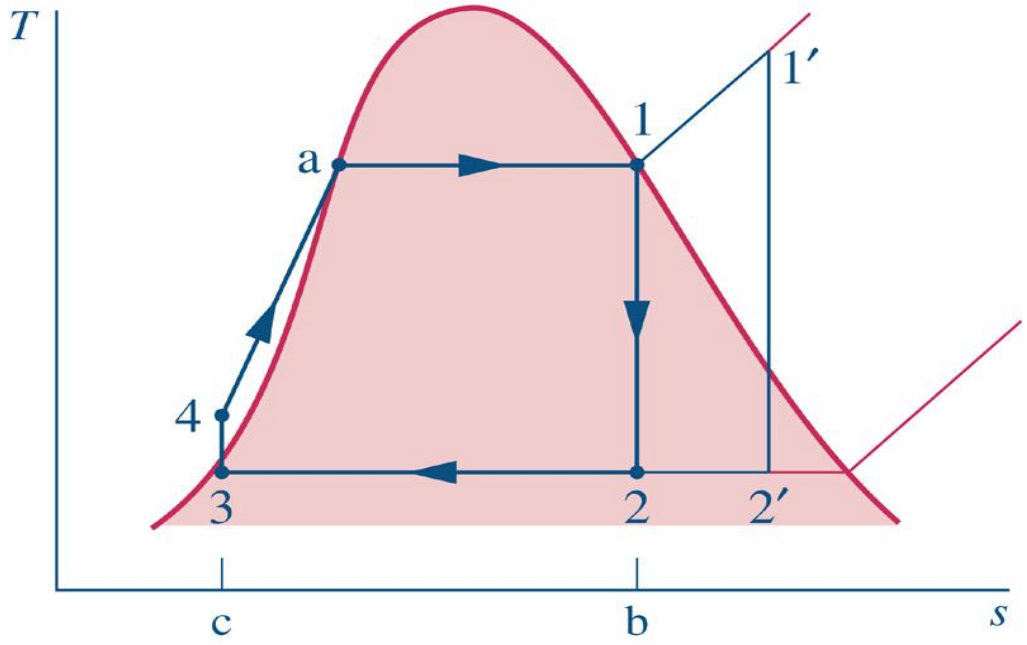

Figure 6: T-s Diagram Showing Effects of Superheating [10]

Figure 4 shows the difference between a regular cycle (noted by 1 and 2) and one that is superheated (noted by 1' and 2'). A regular cycle will only heat the fluid until it is one hundred percent vapor, but still on the vapor dome, before the substance is ran through the expander. As the name implies, the super heated cycle will continue to add energy raising the temperature before the expander is used. The superheating can be controlled by how long the working fluid is kept in the vaporizer of the system.

2.5.2 Open-Loop Pre-Heating

The second configuration that was looked at included three additional pieces of hardware, and the schematic is shown in Figure 7. The open-loop pre-heater is a two expander design that uses partially expanded gas to pre heat the working fluid before it enters the vaporizer. It is called an open-loop system because the gas entering from 2 and the liquid entering at 5 come in direct contact with one another. Since there is open interaction between the two, both the gas leaving the expander and the liquid after pump one need to be at the same pressure. The mass flow rate (y) that travels from the first expander and into the pre-heater can be controlled and optimized. Of all the alternative considerations, this one is the most complex of the three.

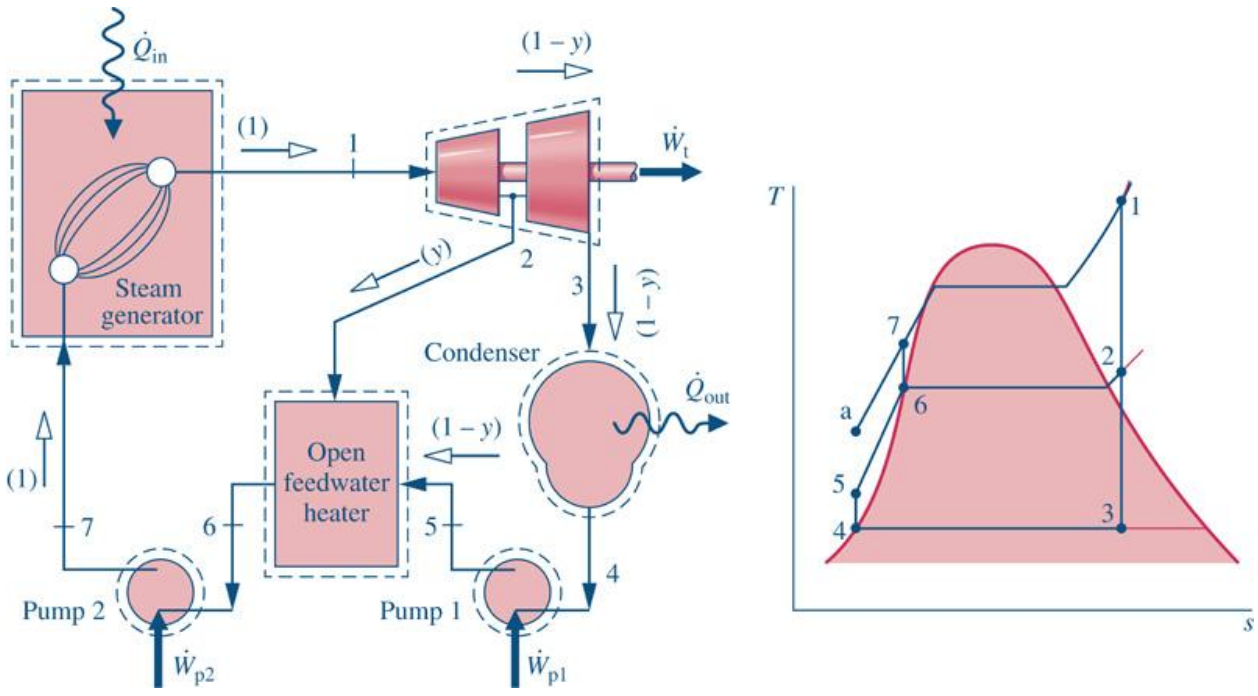

Figure 7: System Configuration and T-s Diagram for Open Loop Pre-Heater [10]

2.5.3 Closed-Loop Pre-Heating

The closed-loop design is a simplified version of the open-loop design. Both use the process of using some of the energy of the expander vapor to pre-heat the working substance before adding the input energy. The only addition to this design is the regenerator, which is a heat exchanger that utilizes excess energy after the expander to preheat the fluid after the pump. The Temperature-Entropy graph in Figure 8 shows that the temperature of the fluid after the expander (5) should equal the temperature of the fluid before entering the vapor generator (3).

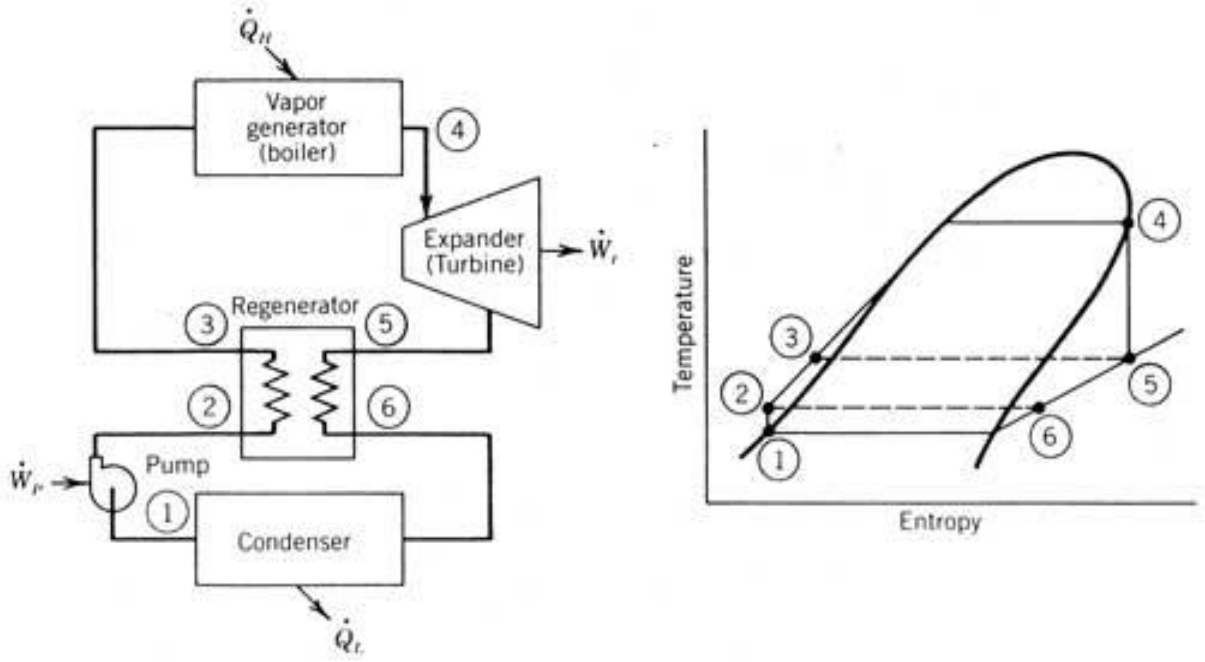

Figure 8: System Configuration and T-s Diagram for Closed Loop Pre-Heating with One Expander

Chapter 3: Results and Discussion of Parametric Study

3.1 R600a (Iso-Butane)

The first organic working fluid that was explored was the refrigerant R600a, also known as iso-butane. The a T-s diagram of the fluid with pressure lines at 1, 5, 10, and 20 Bar is shown below in Figure 9. Iso-butane meets all of the requirements of a working fluid that described in section 2.2 about the fluid selection process. The key feature that made R600a attractive is its low boiling points under reasonable amounts of pressure.

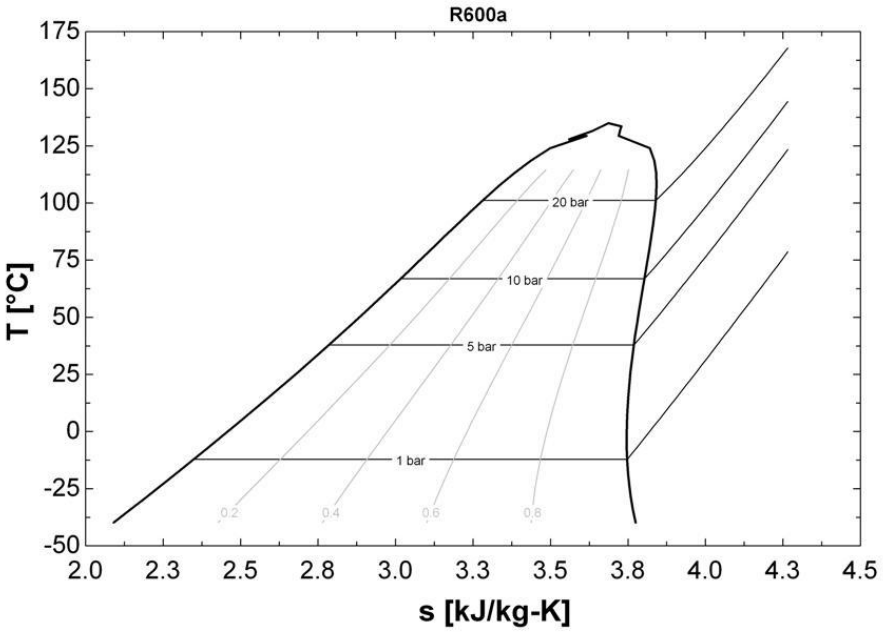

Figure 9: R600a Temperature-Entropy Diagram

Iso-butane is used as the case study to explore the parameters of the regular Rankine cycle that are described in Section 2.1. The three other fluids were also explored in the same manor, but R600a will be discussed in detail in order to give an over view of how the process was performed. For this analysis, the state points are pinned to the vapor dome of the working substance. This means that at the entrance of the expander, the fluid has a quality of 1 (saturated vapor) and prior to entering the pump, it has a quality of zero (saturated liquid).

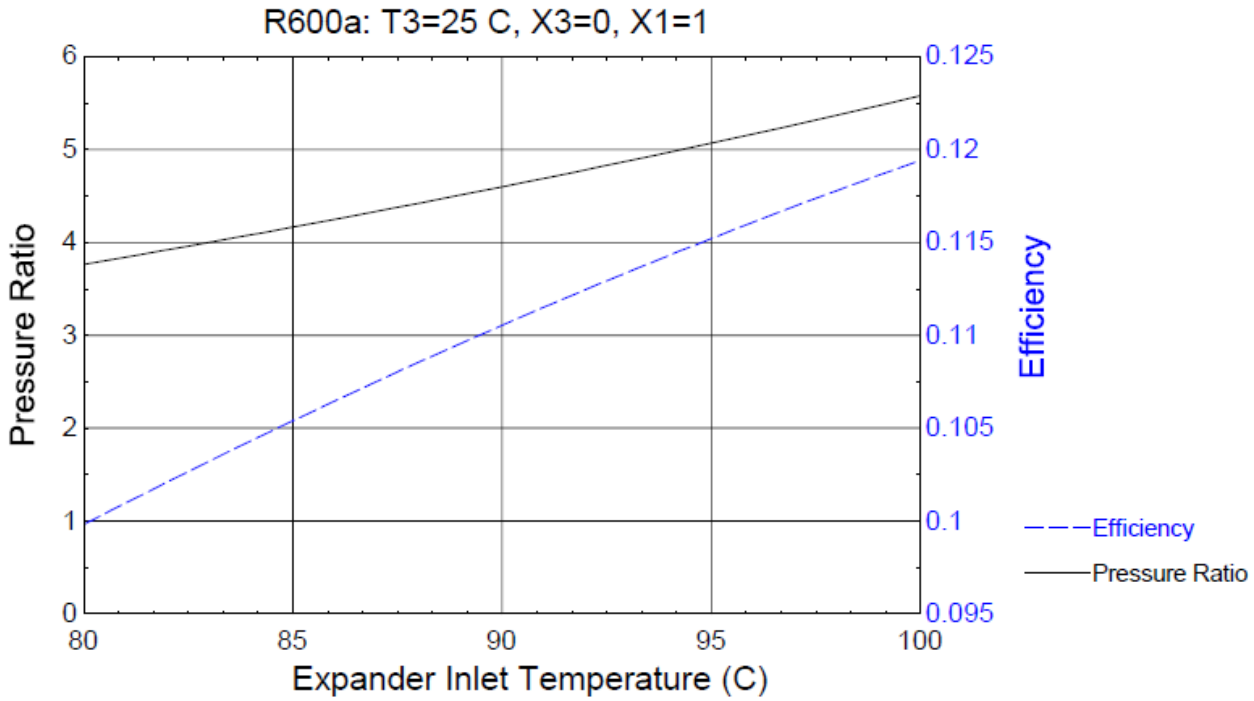

Figure 10: Effect of Expander Inlet Temperature on Pressure Ratio and Efficiency with Fixed Cold Side Temperature

The first parameter that was looked into was the effect of expander inlet temperature. Figure 10 shows a graph to compare how the high side temperature of the cycle affects both the pressure ratio of the expander and the overall efficiency of the system. The graph only explores inlet temperatures up to 101.1° C, which is the vapor dome temperature at the maximum pressure of 20 Bar. Since the cycle is forced to have a quality of zero and low side temperature of 25° C before entering the pump, there is a linear relationship between the pressure ratio of the expander and the inlet temperature. Figure 10 also shows that as the high side temperature continues to increase, the rate at which system efficiency grows trends to slow down.

While Figure 10 above showcases the advantage of raising the inlet temperature of the expander, there are always drawbacks to consider. Figure 11 shows the effect that the increasing the inlet temperature has on the inlet pressure of the expander. The increased inlet pressure requires a more expensive hardware in terms of the expander design.

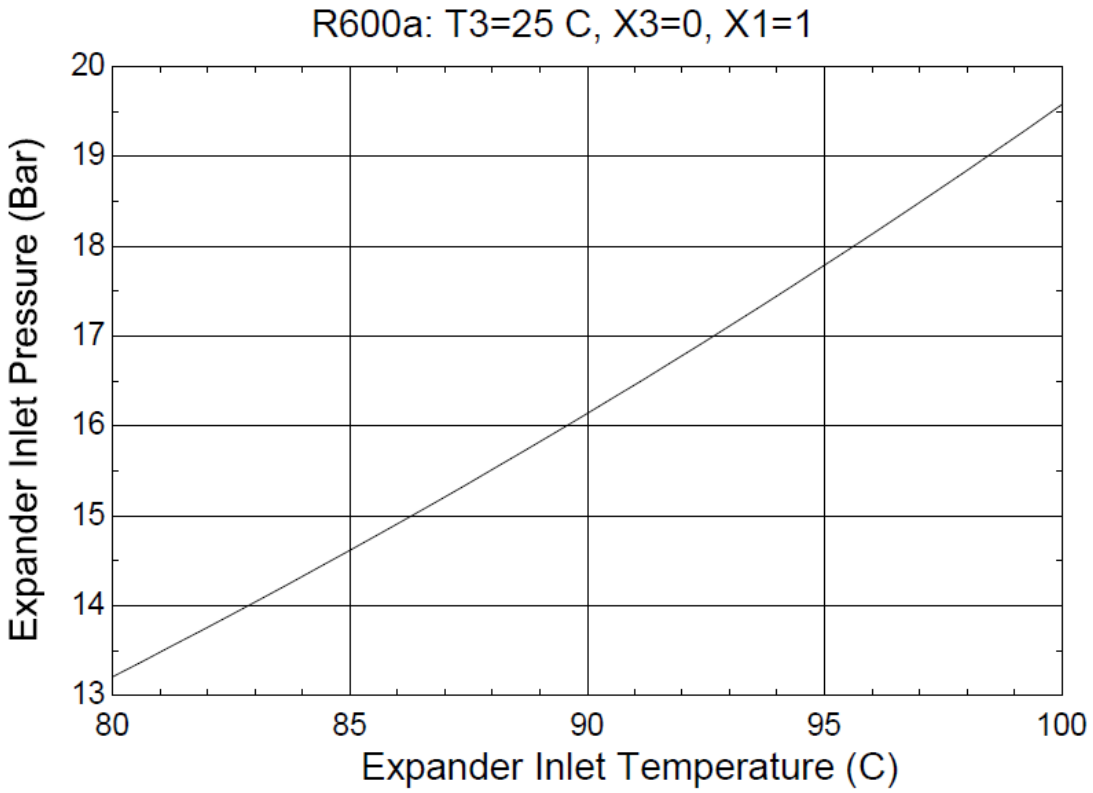

Figure 11: Effect of Expander Inlet Temperature on Inlet Pressure with Fixed Cold Side Temperature

The next parameter of the normal rankine cycle that was investigated was the cold side temperature of the system. Unlike the high side temperature, which can be controlled better by varying how long the fluid is in the solar collector, the low side temperature will be heavily dependent on ambient conditions. Figures 12 and13 show that for the best results, it is important to keep the cold side of the cycle as low as possible. Both the overall efficiency and net work produced by the expander decrease linearly as the low side temperature increases. The only benefit that there is to having a heat sink at a higher temperature is the decreased expander ratio as shown in Figure 13. This added benefit of a lower pressure ratio only keeps the manufacturing process of the expander simple, but the negative effects on the overall system are not justified.

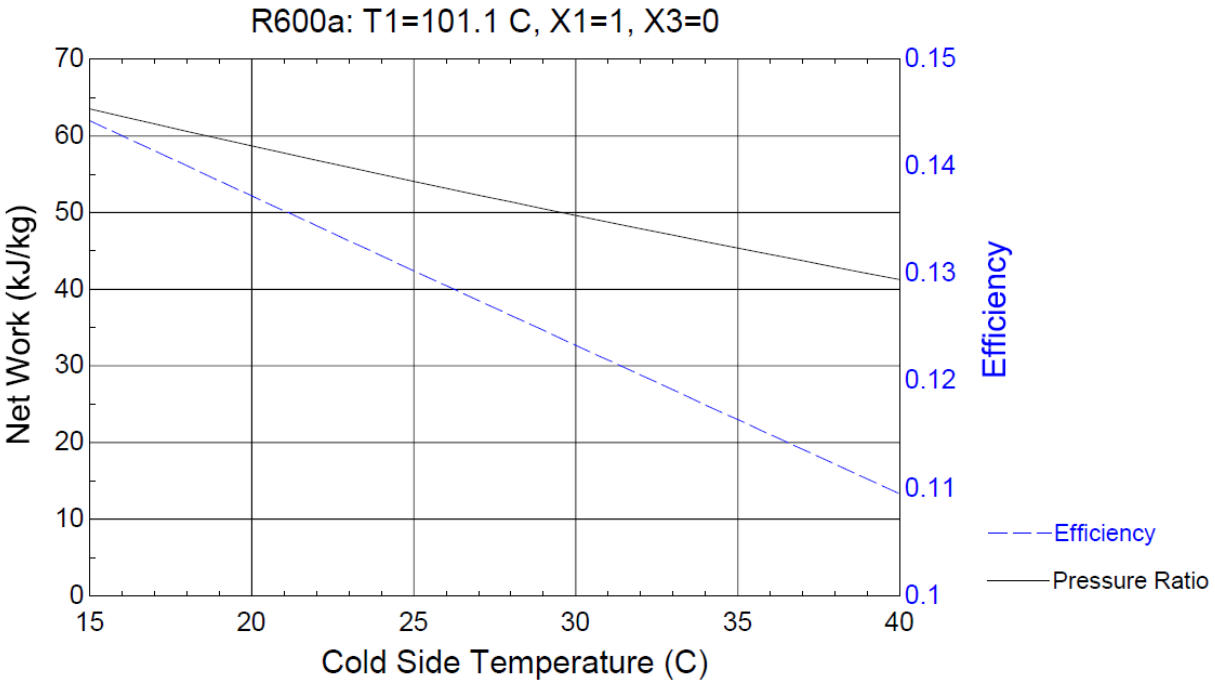

Figure 12: Effects of Cold Side Temperature on System Efficiency and Net Work

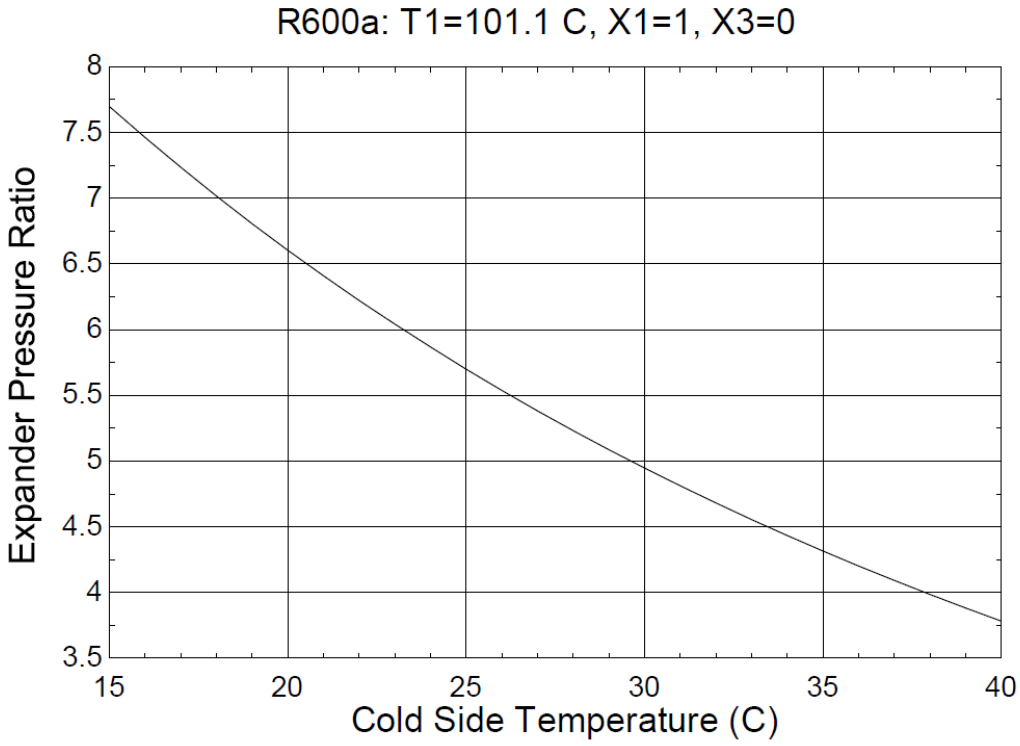

Figure 13: Relationship between Pressure Ratio and Cold Side Temperature

The last input of the regular Rankine cycle to be varied was the high side pressure at the inlet of the expander. For the graph shown in Figure 14 below, there was a set pressure ratio of five for the expander and the input pressure was varied from 13 to 20 Bar to keep within the original system parameters set in section 2.1. The graph shows that for a fixed pressure ratio with the states pinned to the vapor dome, the inlet pressure has an almost negligible effect on the net work and efficiency of the cycle.

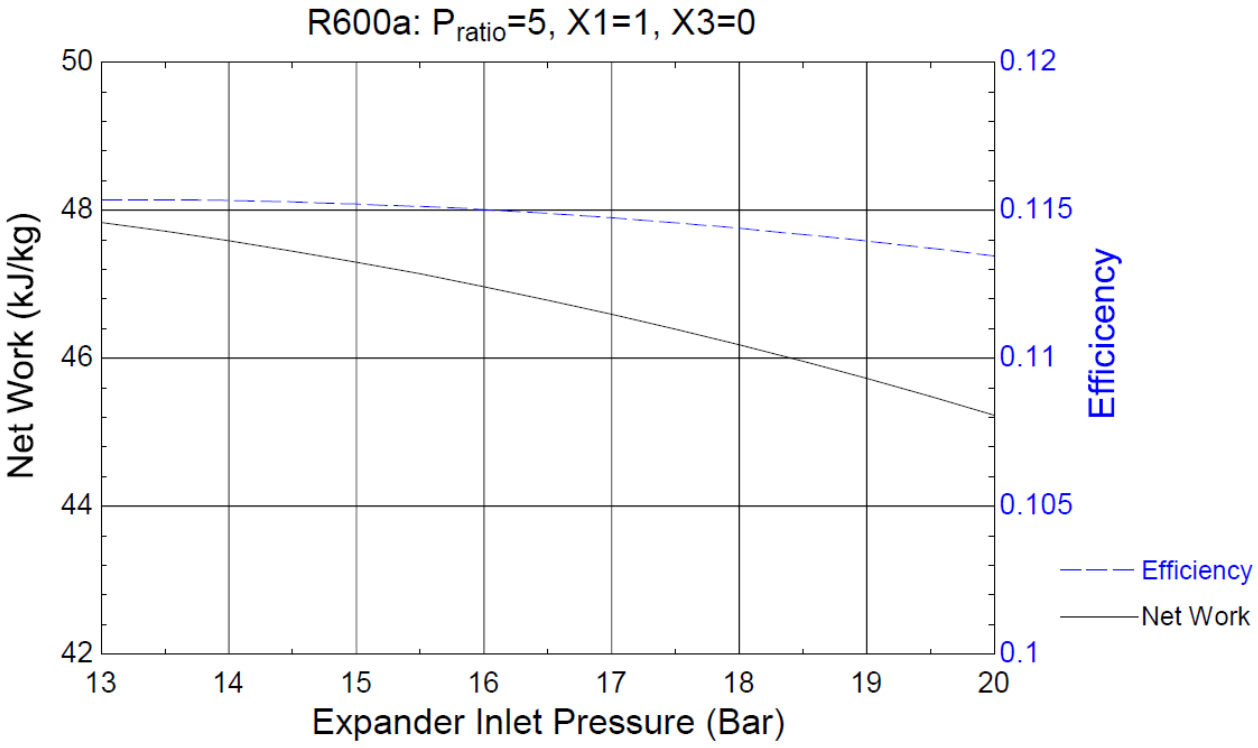

Figure 14: Effects of Expander Inlet Pressure on Efficiency and Net Work with Fixed Pressure Ratio

Although the inlet pressure has next to effect on the cycle for a fixed pressure ratio, if instead the cold side temperature is fixed and the pressure ratio is allowed to vary, the expander inlet pressure plays a much more integral role. Figure 15 shows that as the inlet pressure increases, there is a direct linear correlation to the expander pressure ratio. There is also an exponential relationship between the inlet pressure and the efficiency of the cycle. The figure demonstrates that the most influential factor on the regular Rankine cycle is the expander ratio.

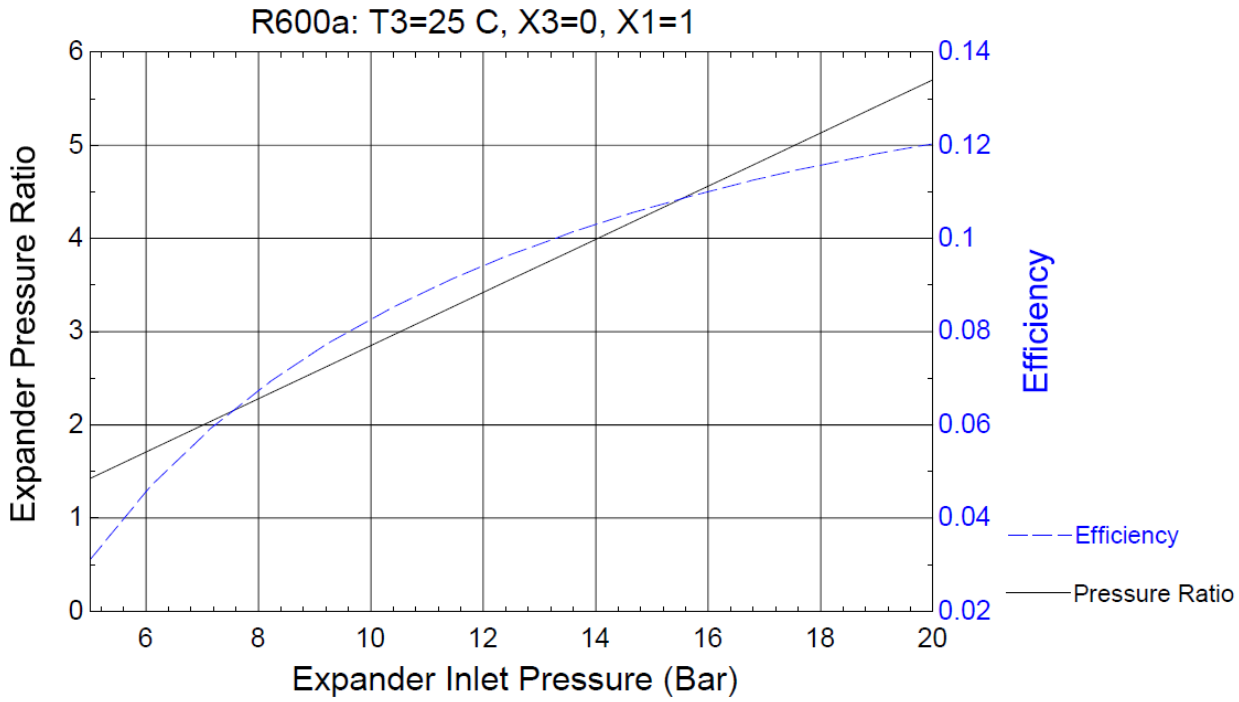

Figure 15: Effects of Expander Inlet Pressure on Efficiency and Pressure Ratio with Fixed Cold Side Temperature

As mentioned in the Section 2.5.1, superheating the fluid beyond the vapor dome is the simplest alternative configuration of a normal Rankine cycle to potentially improve cycle efficiency. To explore effects of superheating on the cycle, the cold side temperature was set to 25° C and pinned to the vapor dome and the expander ratio was varied from 1.5 to 6. What was meant by superheating was raising the temperature of the substance an additional 25° C past the

evaporation temperature. At 20 Bar the vapor dome temperature of iso-butane is 101.1° C, this means for superheating the inlet temperature of the expander would be set to 126.1° C.

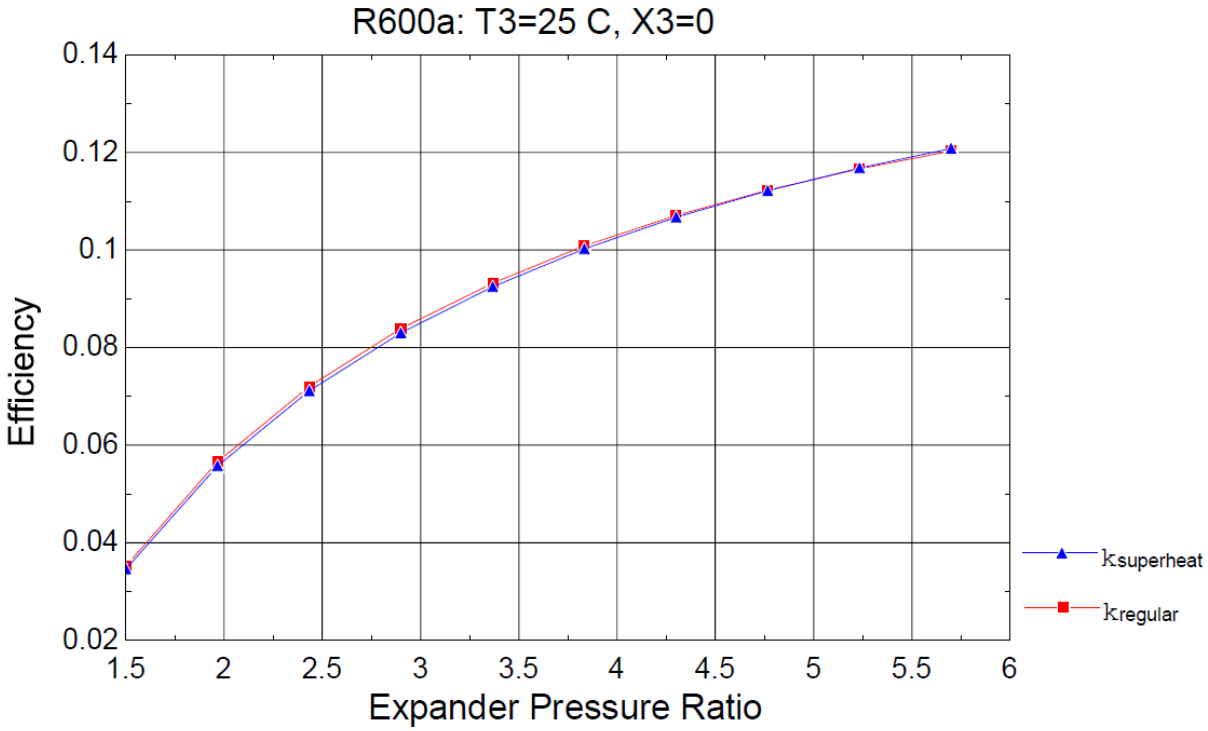

Figure 16: Effects of Superheating Fluid by 25 C on System Efficiency, As a Function of Expander Pressure Ratio

Figure 16 shows the effects of superheating the fluid 25° C past the vapor dome temperature. The graph shows that both the regular Rankine cycle in red, and the superheated version in blue follow the same trends. The interesting thing is that for iso-butane, there is nominally no gain in efficiency achieved by superheating. This is due to the shape of the vapor dome for iso-butane which is different form steam (water) where gain in efficiency by superheating is expected. This is promising since the input of the cycle is low grade heat from the solar collectors.

In order to validate that there are no added efficiencies with allowing the fluid to be superheated, a second numerical analysis was preformed. In the last parametric study, the fluid was on heated 25° C past the vapor dome. Here the working substance was looked at for a range

of superheated values. The expander pressure ratio was fixed at 5 and the inlet pressure of the expander was set to 15 Bar which corresponds to a vapor dome temperature of 86.3° C. In Figure 17 below, the inlet temperature was varied from 86.3°C all the way up to 200° C. The graph shows that the higher the inlet temperature is superheated, the less efficient the cycle becomes. The only added benefit of the superheating process is the increased net work per unit mass of the working fluid that the system produces.

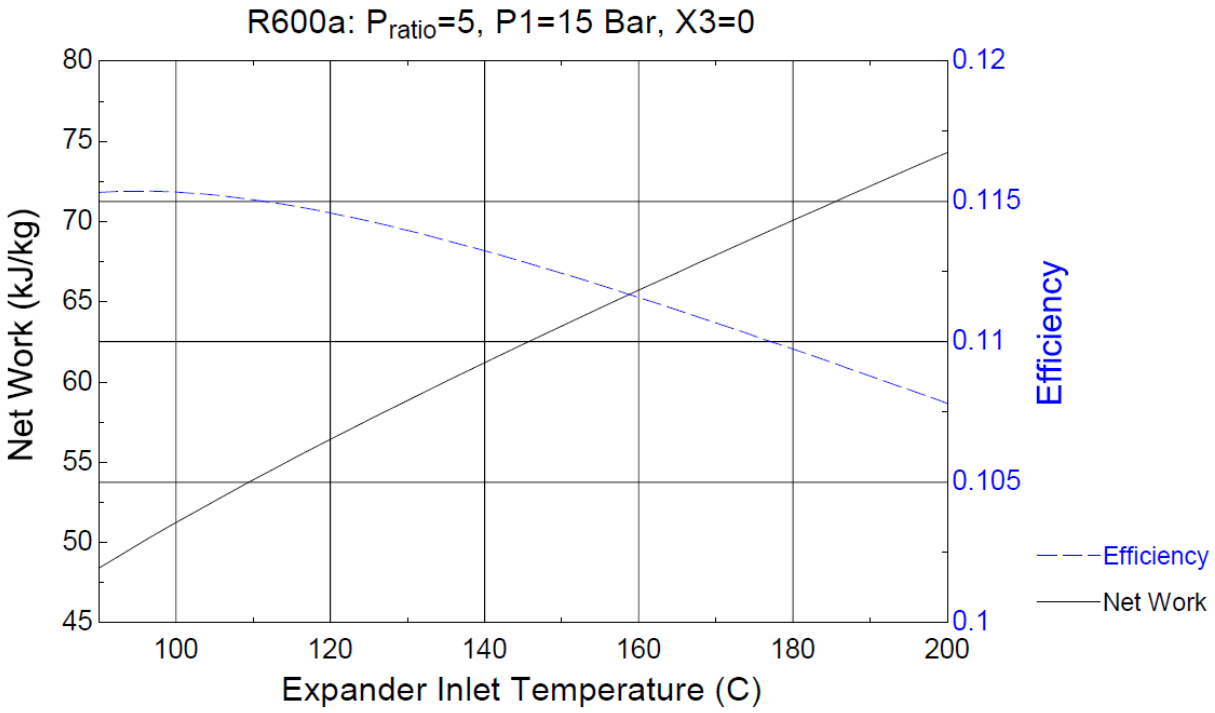

Figure 17: Effects of Excess Superheating on Net Work and System Efficiency

There were several variables that were parametrically explored to get a good understanding of how each variable effect the overall Rankine cycle. Table 4 on the next page gives a summary of how each input variable positively or negatively affects the output of the cycle. In some cases, like the inlet temperature of the expander, the variable can have both favorable and negative changes associated with their variations.

Table 6: Summary of Regular Rankine Cycle Exploration for Iso-Butane

Parameter to be Explored	Effects on the System
Expander Inlet Temperature No Superheating	There is linear relationship between the inlet temperature and the system efficiency and pressure ratio of the expander. As expander inlet temperature increases, so will the efficiency and pressure ratio.
Expander Inlet Temperature Superheating	For the selected fluids, there is no benefit to superheating the fluid off the vapor dome. There is actually a loss in efficiency due to superheating.
Expander Inlet Pressure	There is an exponential relationship between inlet pressure and system efficiency that approaches an asymptote at higher pressures. This means there is originally a strong dependence on inlet pressure that will eventually level off.
Expander Pressure Ratio	Of all the parameters, the expander ratio has the largest influence on the efficiency of the system
Bottom Condenser Temperature	There is a linear relationship that shows the lower the bottom side temperature source, the higher the overall system efficiency.

While Table 6 above gives a good verbal description of how the different parameters affect the overall system, EES can create 3D plots that graphically represent the information in the table. Each of the 3D plots that follow represents efficiency as a function of expander inlet temperature and pressure ratio with a fixed expander inlet pressure. The cold side temperature of the system will determine how large of an expander pressure ratio the system can accommodate. Table 7 below gives a listing of the maximum pressure ratios that the cycle can have depending on the inlet pressure of the expander and the condensing temperature of the cold side.

Table 7: Maximum Expander Pressure Ratio for Given Inlet Expander Pressure and Minimum Cold Side Temperature for R600a

	Maximum Expander Pressure Ratio					
Inlet Pressure [Bar]	T3=40 C	T3=35 C	T3=30 C	T3=25 C	T3 = 20 C	T3 = 15 C
20	3.784	4.317	4.948	5.702	6.607	7.7
15	2.838	3.237	3.711	4.276	4.955	5.775
10	1.892	2.158	2.474	2.851	3.303	3.85
5	N/A	1.079	1.237	1.425	1.652	1.925

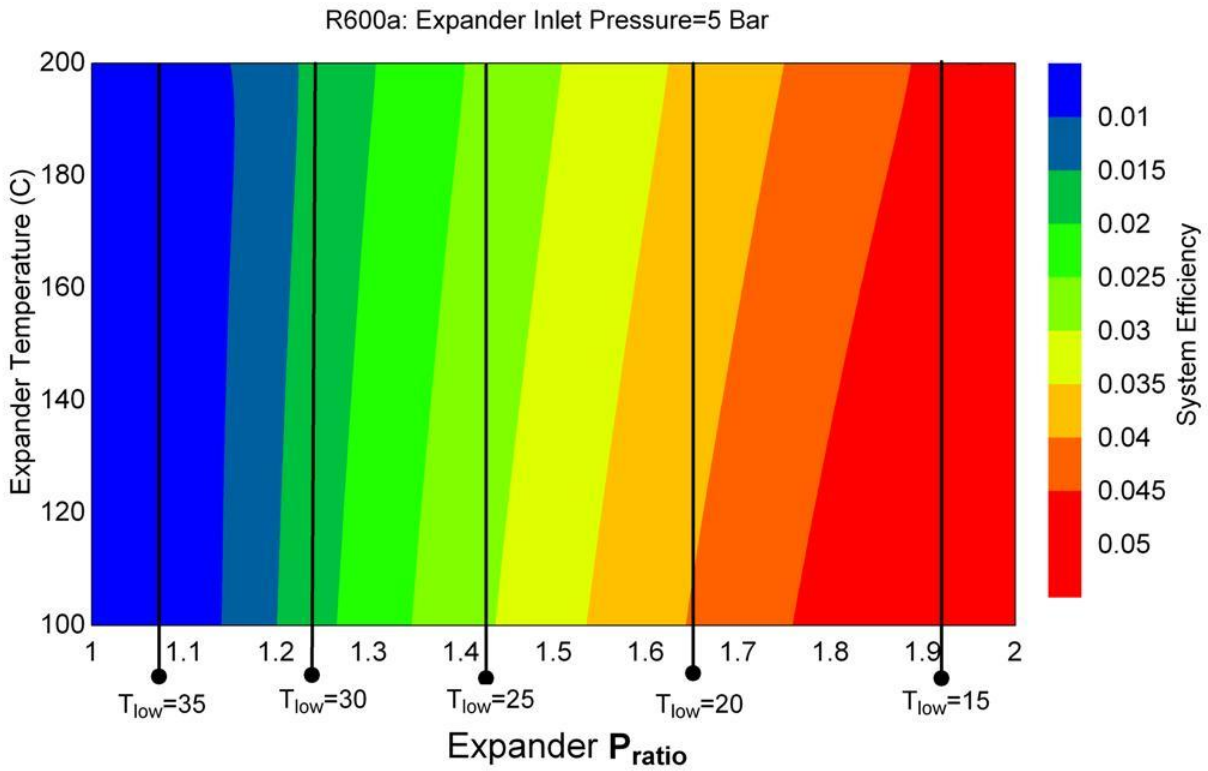

Figure 18: R600a System Efficiency Plot for Varying Expander Inlet Temperatures and Pressure Ratio, with Inlet Pressure of 5 Bar

Figure 18 combines all of the parameters of the regular Rankine cycle. The x-axis varies the expander pressure ratio from 1 to 2 which is representative of the maximum values found in Table 7. The y-axis represents the inlet temperature of the expander and looks at the effects of superheating. The efficiency is shown as a color map and the color scale is displayed to the right of the graph. The vertical lines with the dot on the end represent the maximum pressure ratios that correspond to the available condenser temperature. As noted in the title of the graph, Figure 15 is an exploration of a system with an expander inlet pressure of 5 Bar.

All of the effects of the different input parameters that were mentioned earlier are graphically summarized in the figure. As the expander pressure ratio gets larger, the efficiency of the system increases. The lower the cold side temperature allows from larger pressure ratios and thus higher efficiency. As the fluid is superheated, the curve of the efficiency shows that higher temperatures do not increase the efficiency of the cycle.

Figures 19-21 are very similar graphs expect for the inlet pressure of the expander. The graphs still vary the same parameters in order to look at the efficiency of the system. Figures 19 and 20 have an additional dashed line that signifies another limiting factor of the cycle. The line represents the vaporization temperature of the working fluid at the give inlet pressure. At 15 and 20 bar, the lowest possible inlet temperature are 88.3° C and 101.1° C, respectably. Any expander inlet temperature set below that value will not have enough energy to create a phase change in the substance. As the graph shows, when the inlet temperature is close to the vaporization line, the trends of the graph become erratic and the data below this should be ignored.

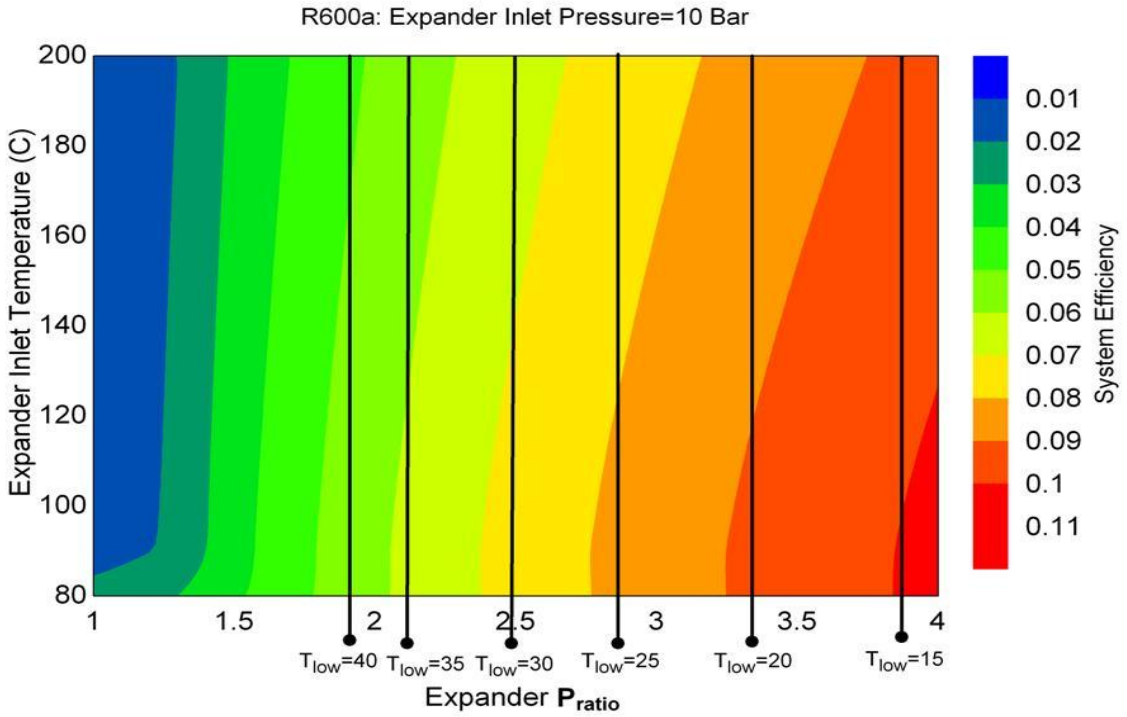

Figure 19: R600a System Efficiency Plot for Varying Expander Inlet Temperatures and Pressure Ratios, with Inlet Pressure of 10 Bar

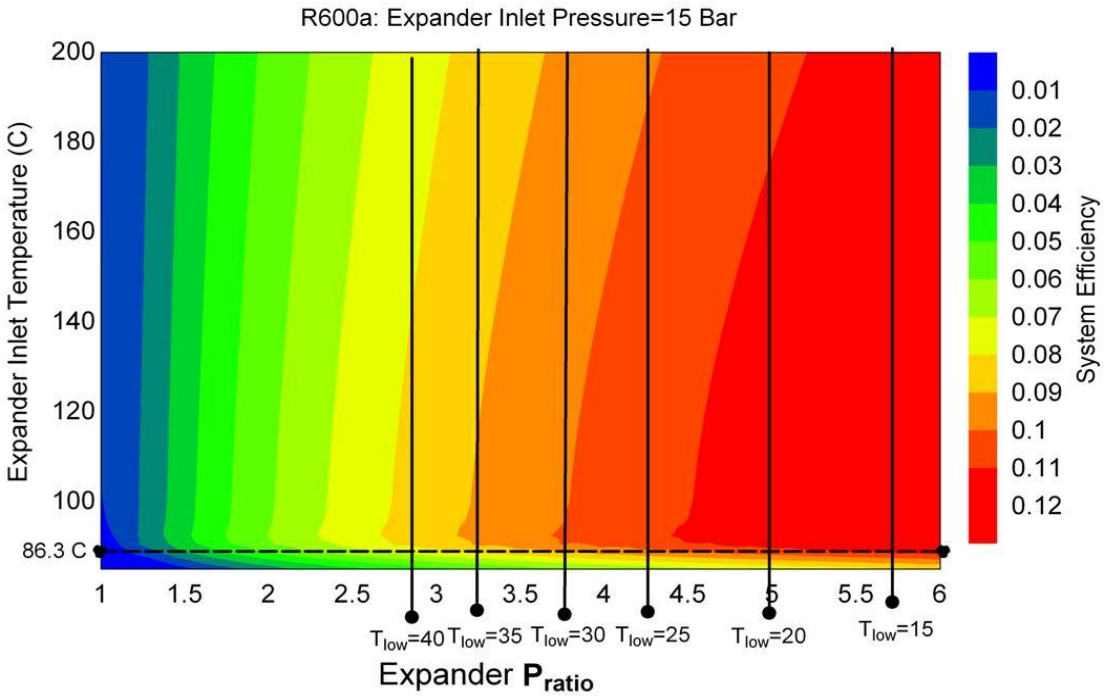

Figure 20: R600a System Efficiency Plot for Varying Expander Inlet Temperatures and Pressure Ratios, with Inlet Pressure of 15 Bar

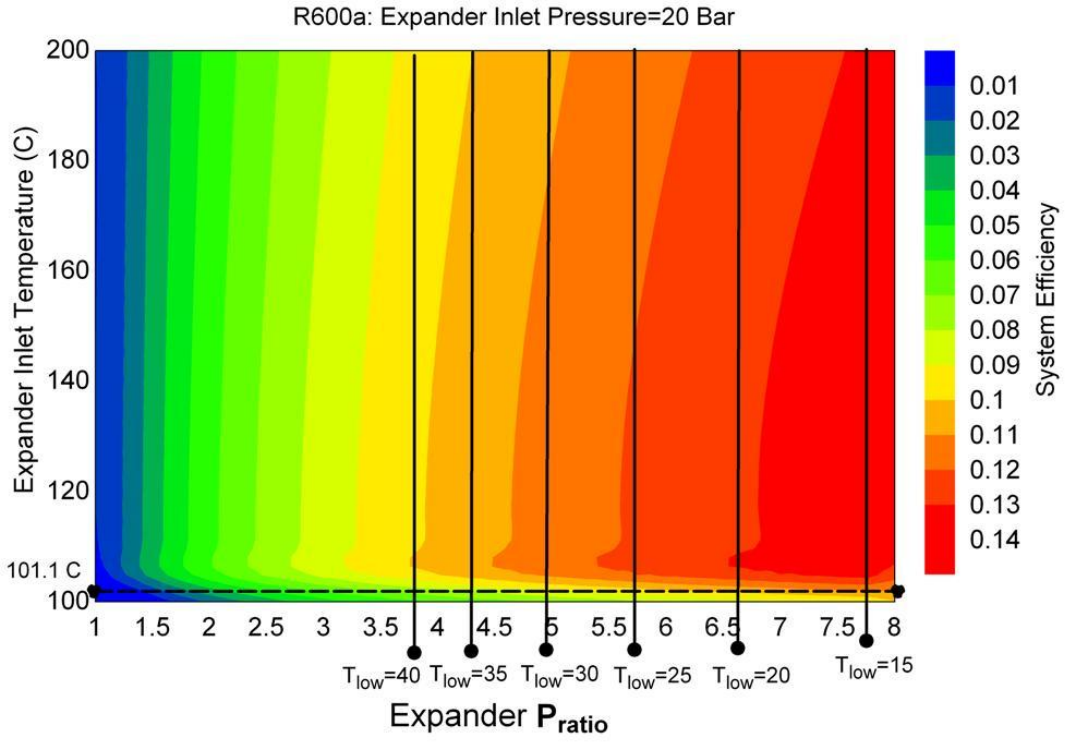

Figure 21: R600a System Efficiency Plot for Varying Expander Inlet Temperatures and Pressure Ratios, with an Inlet Pressure of 20 Bar

After the effects of superheating were explored for a regular Rankine cycle, the next configuration to be investigated was the closed loop pre-heater that was described in Section 2.5.3. For this pre-heating design, both the regular and the superheated cycle were taken into account. Figure 22 below gives a visual representation of how the closed loop design effects

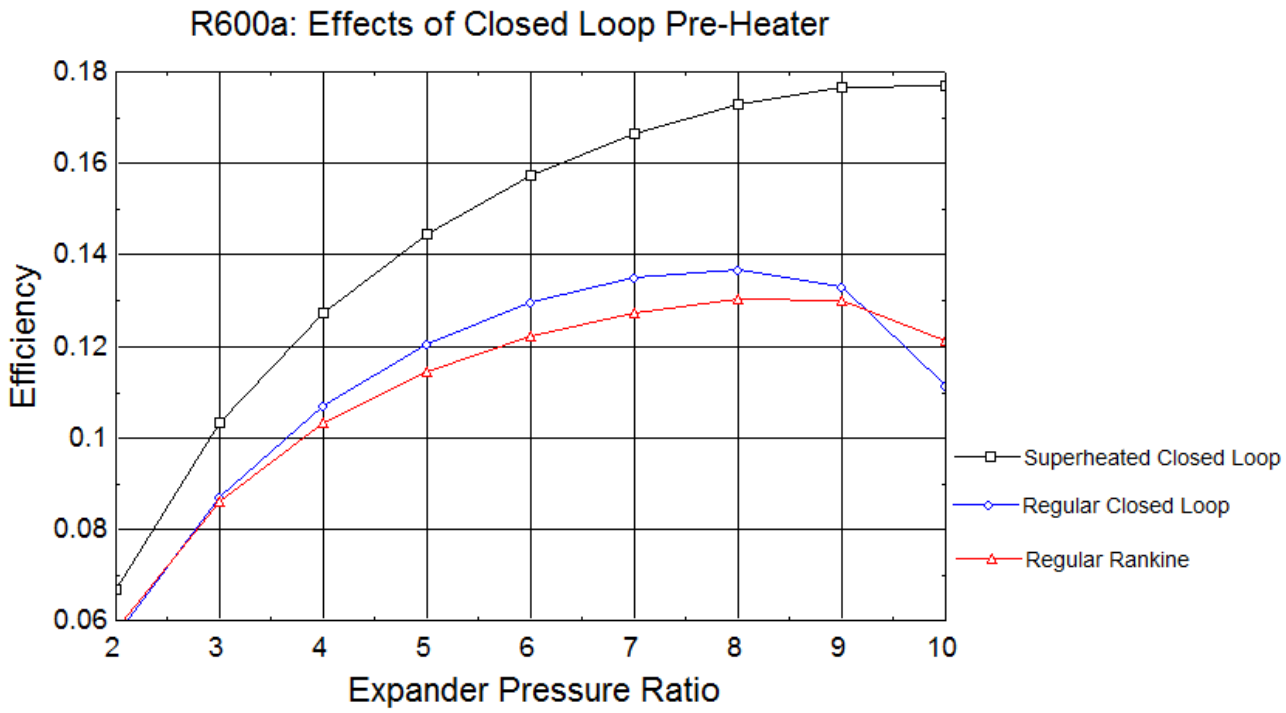

Figure 22: Effects of Superheating Fluid by 25 C on System Efficiency, Over Range of Expander Pressure Ratios for a System with Closed Loop Pre-Heating

the overall system efficiency. The graph looks at three different scenarios: a regular Rankine cycle, a closed loop pre-heating design with no superheating, and a closed loop pre-heating design with superheating. For this study, the cold side was held at 25° C with a quality of zero. As the figure shows, there is very little improvement in system efficiency from the regular Rankine cycle to a closed loop with no superheating. The real advantage of the pre-heater design can only be seen when superheating is involved. When the fluid is superheated 25° C above the evaporation temperature the excess energy greatly increases the system efficiency.

The final system configuration that was considered was the open loop pre-heater design. As discussed in Section 2.5.2, in order to utilize this design, an additional pump and expander must be implemented. A simulation was run to see if the added benefits on system efficiency outweigh the cost associated with the extra hardware. With an inlet pressure of 20 Bar, temperature of 101.1°C, and a cold side temperature of 20° C, the pressure after the first expander was varied to look at the optimum pressure ratios for system efficiency and net work.

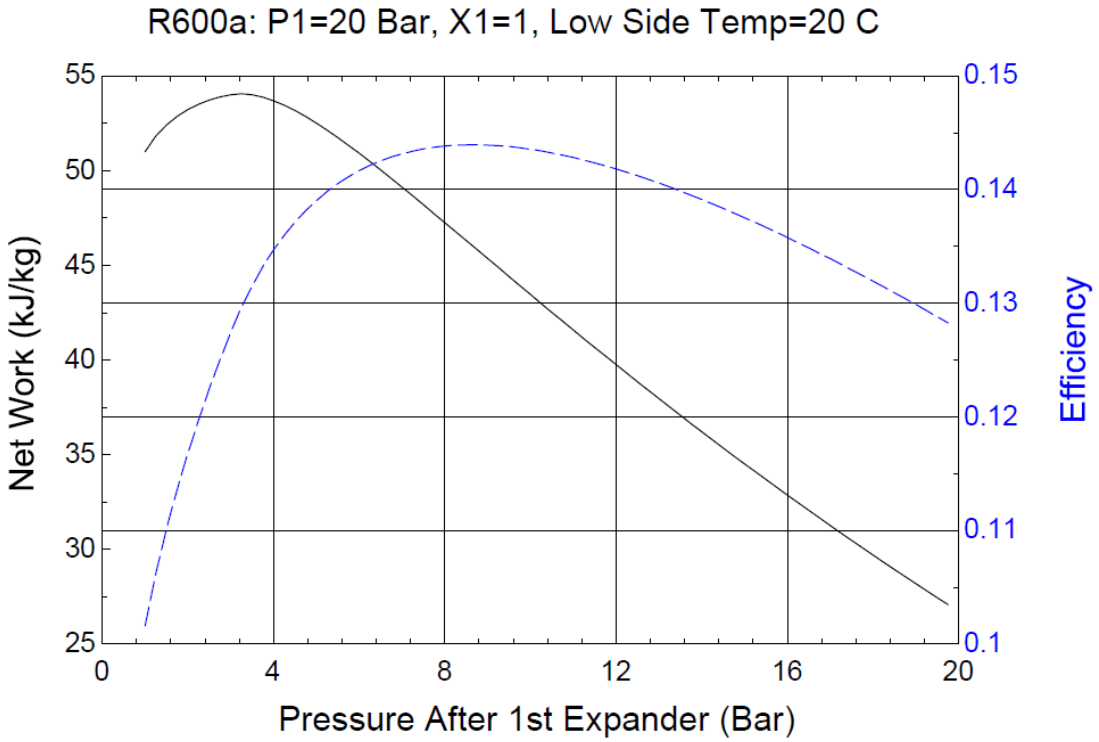

Figure 23: Effect of Open Loop Pre-Heater on R600a

Figure 23 shows the effects of varying the outlet pressure of the first expander, and there is an optimal value of 8.2 Bar or an expander ratio of 2.45. Under those conditions, it was found that a system efficiency of 14.4% could be achieved. Now when an ordinary Rankine cycle is run with the same high and low side conditions, and efficiency of 12.8% was possible. The costs of adding an additional expander to the system will almost double the overall price and it was determined that the extra 1.6% of system efficiency was not worth further exploration.

3.2 n-Pentane

The second working fluid that was explored in depth is n-pentane. The substance is an organic fluid, and it shares many similarities with iso-butane. Both fluids phase change in the desired regions and have T-s curves that slope inward on the gaseous side as shown in Figure 24 below.

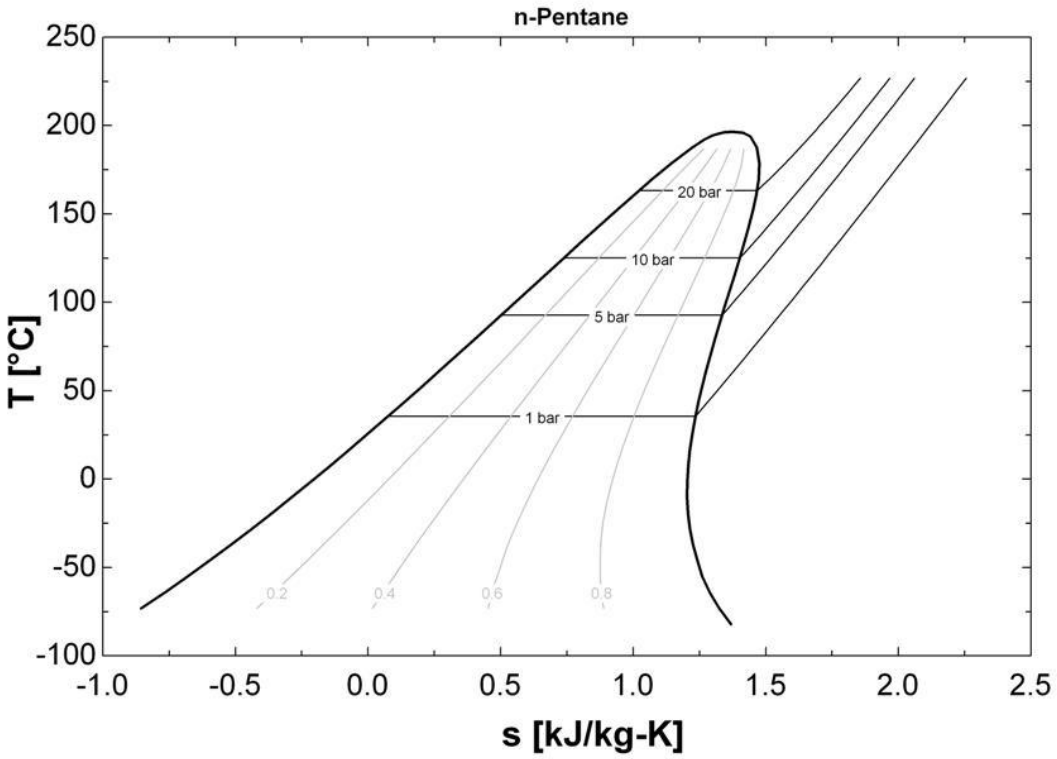

Figure 24: n-Pentane Temperature-Entropy Diagram

The same parametric study that was completed for iso-butane was also preformed on n-pentane as well as the other two fluids (methanol and ethanol). Because of the similarities in thermodynamic properties of the two fluids, the trends of the regular Rankine cycles were similar and will not be discussed in detail. The same treads that were documented in Table 6 for R600a hold true for n-pentane.

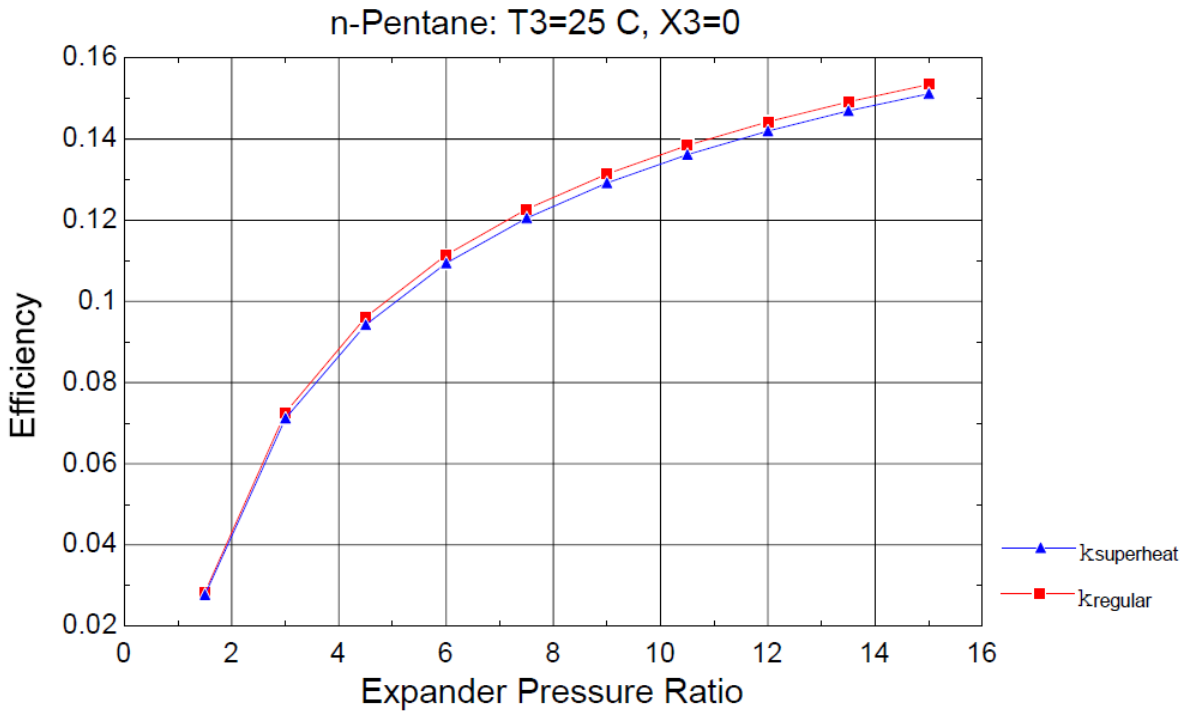

Figure 25: Effects of Superheating n-Pentane by 25 C on System Efficiency

When exploring the effects of superheating a four stage Rankine cycle, the results found directly echo what was found with iso-butane. As Figure 21 shows, when the fluid is superheated an additional 25° C past the vaporization temperature, the system actually loses efficiency across a range of pressure ratios. Like with R600a, this is due to the shape of the T-s diagram.

3-D plots for n-pentane were generated in the same fashion that the graphs for iso-butane were created. Only the graphs with inlet pressures of 10 and 20 Bar have been included to give a representation of the range of system efficiencies that are available. Table 8 breaks down the maximum pressure ratios that are associated with the different cold side temperatures.

Table 8: Maximum Expander Pressure Ratio for Given Inlet Expander Pressure and Minimum Cold Side Temperature for n-Pentane

	Maximum Expander Pressure Ratio					
Inlet Pressure [Bar]	T3=40 C	T3=35 C	T3=30 C	T3=25 C	T3 = 20 C	T3 = 15 C
20	17.19	20.34	24.21	29.02	35.04	42.64
15	12.9	15.25	18.16	21.76	26.28	31.98
10	8.597	10.17	12.1	14.51	17.52	21.32
5	4.299	5.084	6.052	7.254	8.76	10.66

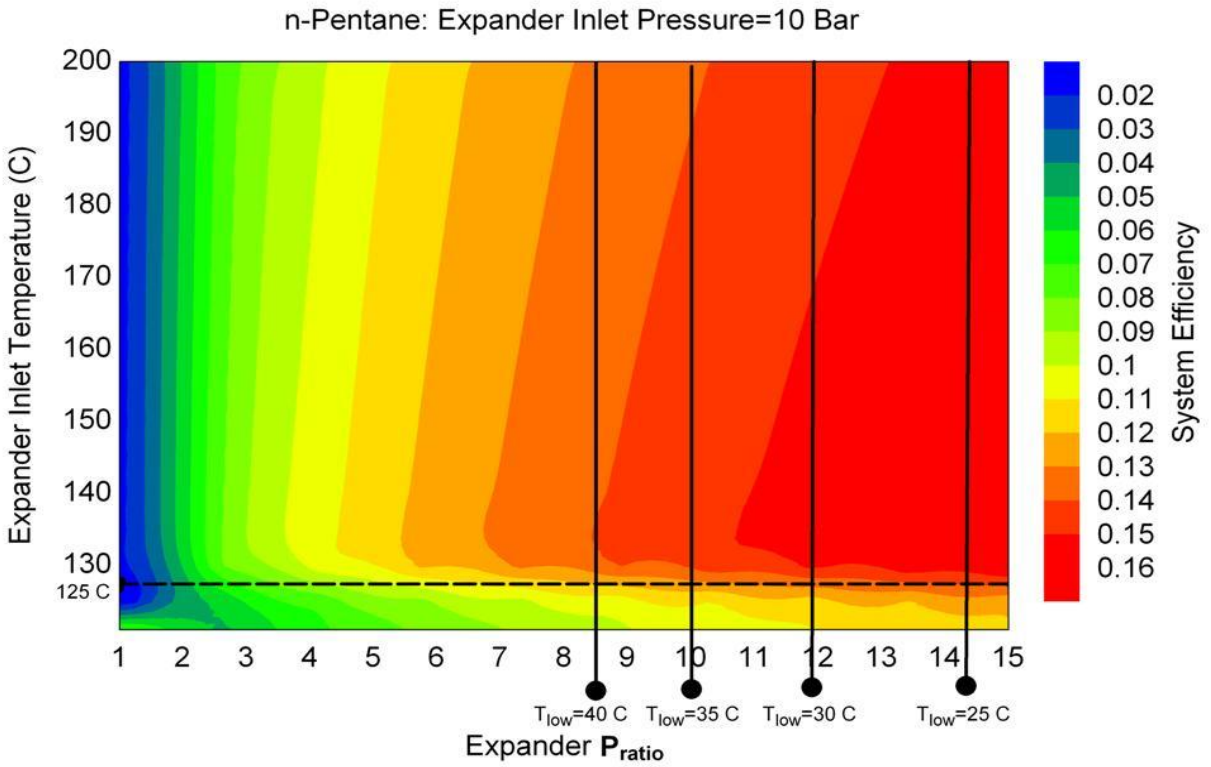

Figure 26: n-Pentane System Efficiency Plot for Varying Expander Inlet Temperatures and Pressure Ratios, with an Inlet Pressure of 15 Bar

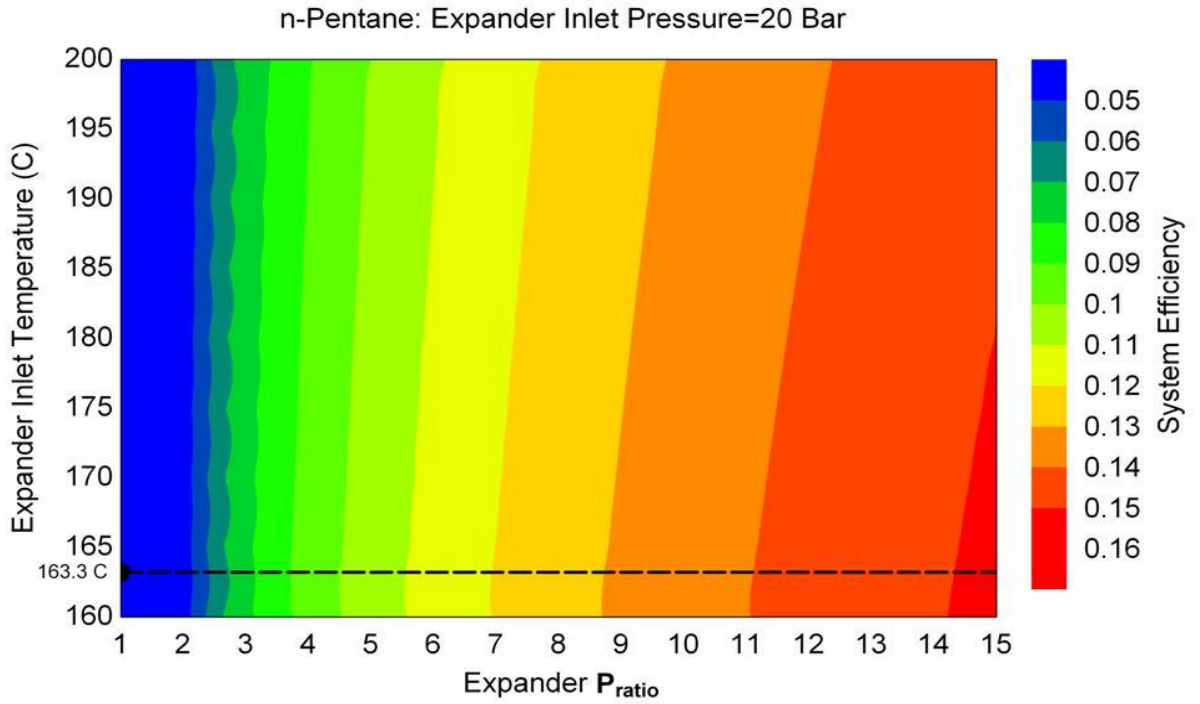

Figure 27:n-Pentane System Efficiency Plot for Varying Expander Inlet Temperatures and Pressure Ratios, with an Inlet Pressure of 20 Bar

Figures 26 and 27 show n-pentane is capable of reaching slightly higher efficiencies than iso-butane. The fluid can experience larger pressure ratios and reach system efficiencies in the upper range of 15-16%. The drawback is the higher vaporization temperatures (dashed lines) that must be surpassed by additional energy.

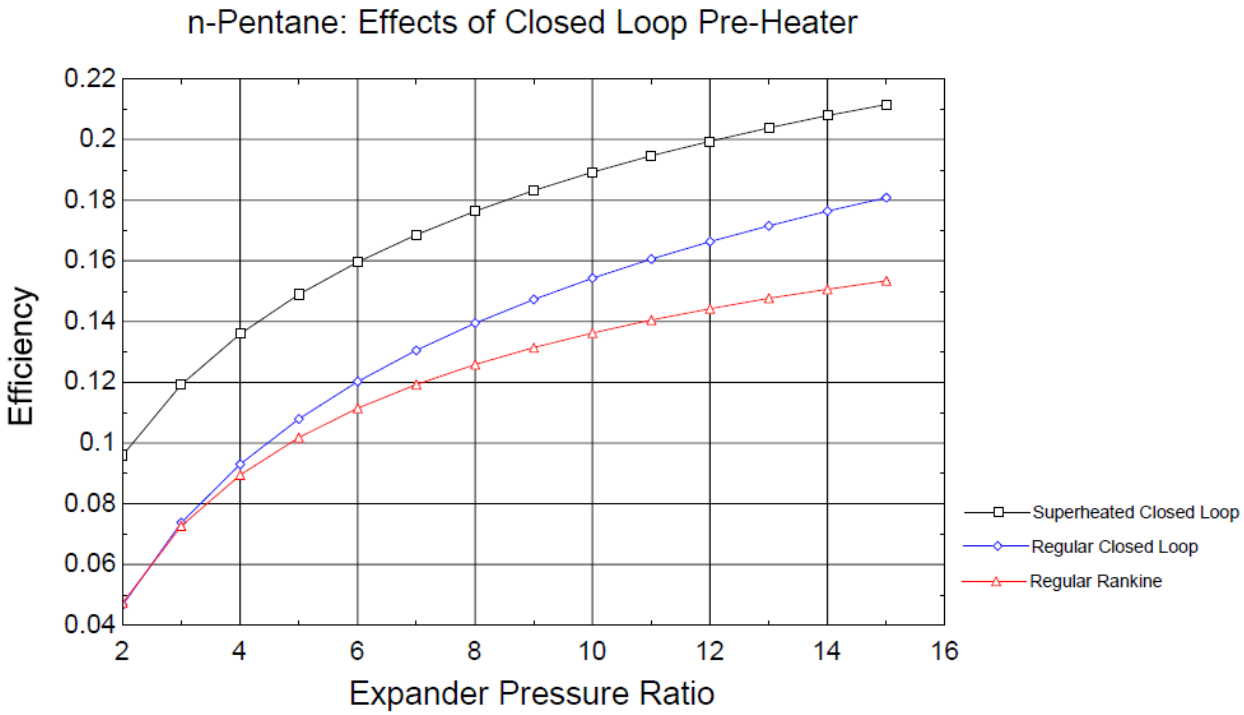

Figure 28: Effects of Closed Loop Pre-Heating with Optional Superheating for n-Pentane

The closed loop pre-heater configuration adds up to an additional six percent to the overall efficiency. As Figure 28 shows, at lower pressure ratios, the benefits of the pre-heater are negligible, but the two start to diverge as the expander ratio increases. There is a consistent gain from the regular closed loop configuration and the superheated design.

3.3 Methanol

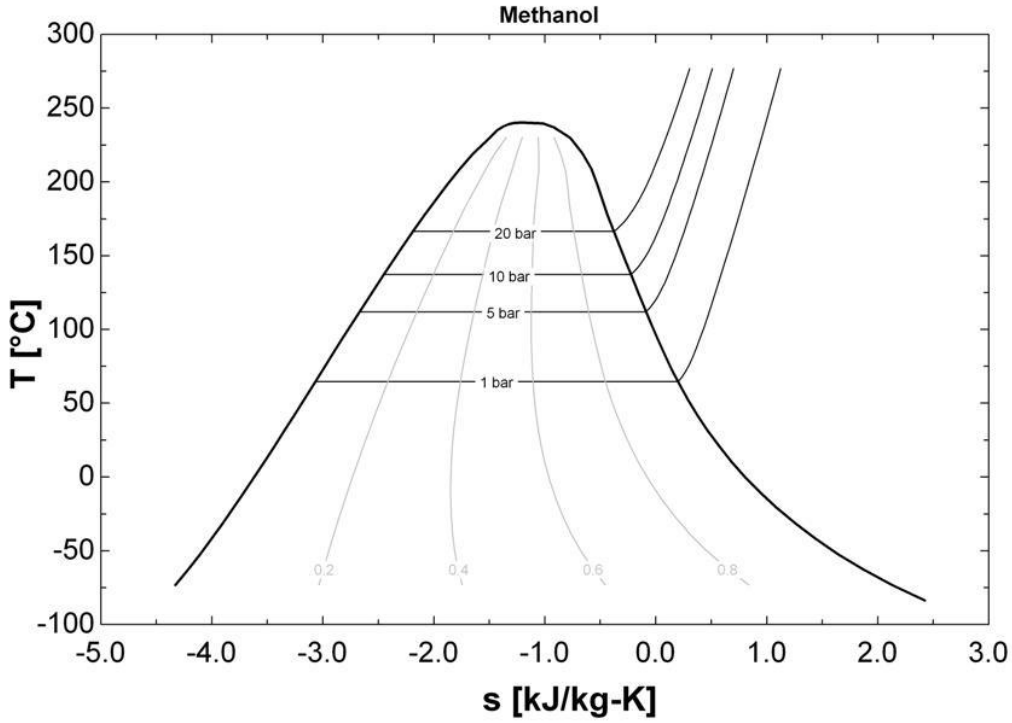

Figure 29: Methanol Temperature-Entropy Diagram

Like iso-butane and n-pentane, methanol exhibits the necessary thermodynamic properties as well as the environmental attributes. However, as shown in Figure 29, the shape of the methanol's T-s diagram doesn't curve in as was the case for the previous substances .Since methanol is an alcohol, there are no concerns with ozone depletion or global warming. Methanol is a commonly available substance that is currently employed for a variety of applications.

The basic Rankine system configuration for methanol was explored and showed the same trends overall trends as the other fluids. However, the superheating of the methanol in a Rankine cycle did produce different results. Although minor, Figure 30 does show that superheating methanol by 25° C has a positive effect on the system efficiency for the range of pressure ratios. To explore the affects of superheating deeper, the pressure ratio was set to 10 and the additional superheating was varied from 0°-110° C. Figure 31 shows an exponential correlation between the degrees of superheating the efficiency of the system.

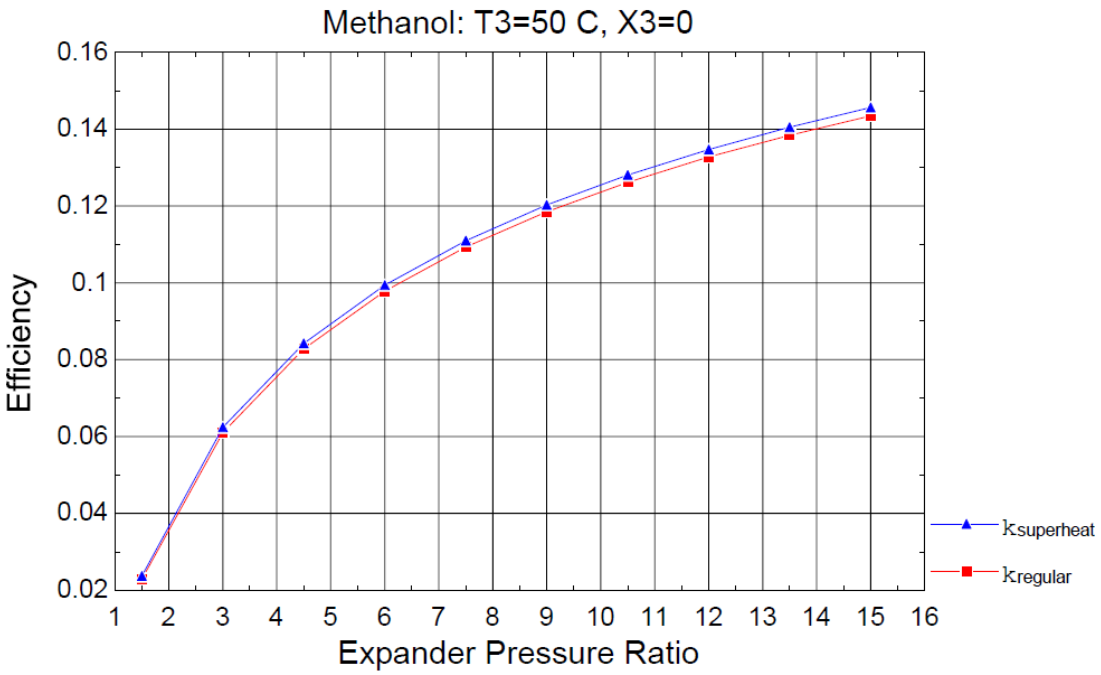

Figure 30: Effects of Superheating Methanol by 25 C on System Efficiency

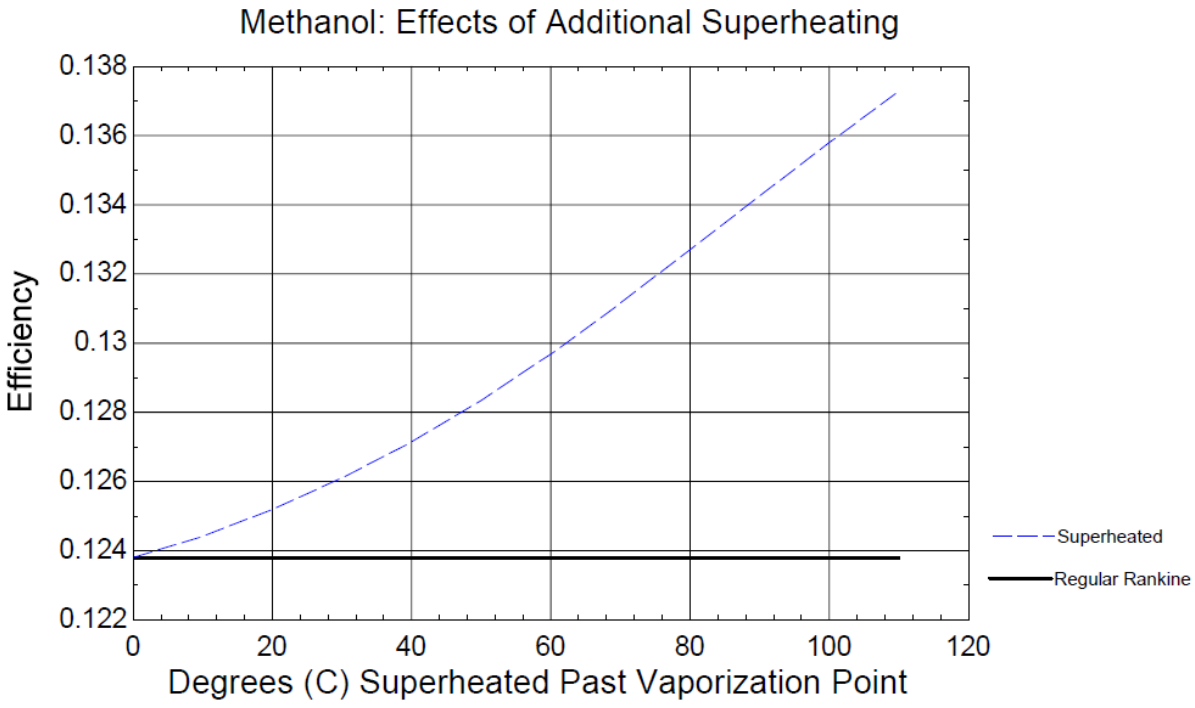

Figure 31: Effects of Superheating Methanol with a Pressure Ratio of 10

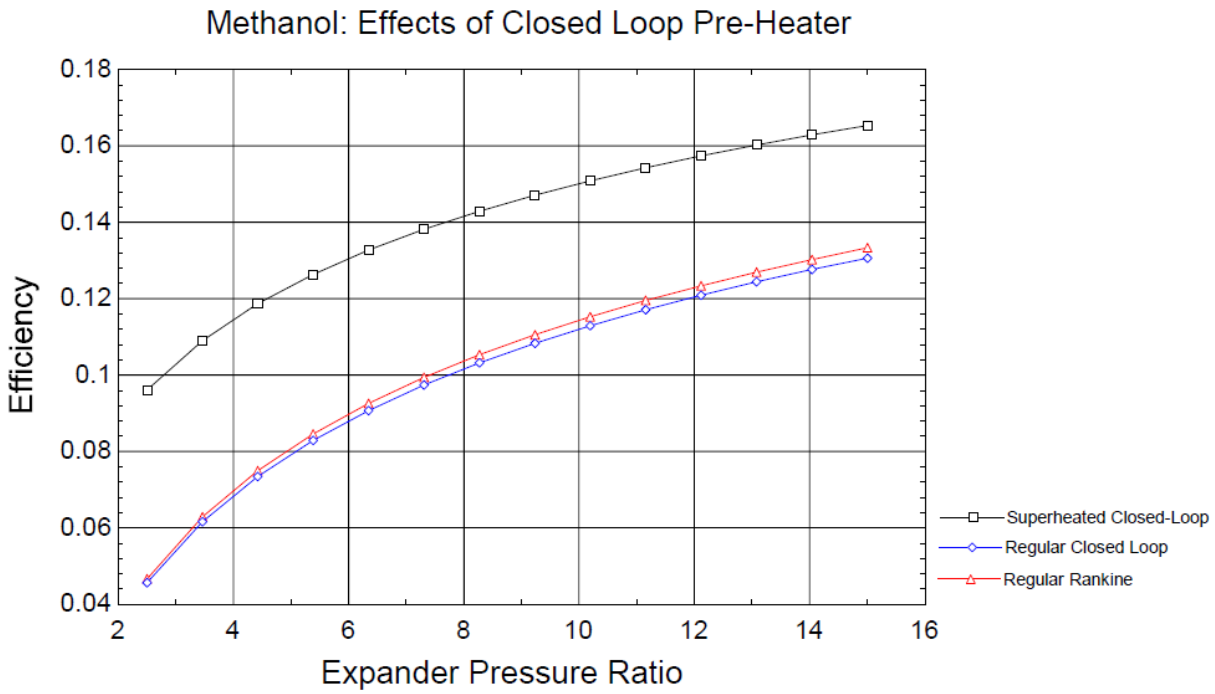

Figure 32: Effects of Closed Loop Pre-Heating with Optional Superheating for Methanol

For methanol, the closed loop pre-heater configuration did not follow the same trends as the other two fluids. As shown above in Figure 28, if there is no superheating involved with the pre-heating design, the system actually loses efficiency as opposed to gaining efficiency. However, when superheating is incorporated, methanol follows the same trend as before.

Figures 33 and 34 show the 3D plots for methanol with inlet pressures of 10 and 20 Bar respectably. The bars on the graph slope to the left signifying that there is efficiency gain when the cycle is superheated. Table 9 shows that the maximum pressure ratios for the varying cold side temperatures are much higher than the range of input values.

Table 9: Maximum Expander Pressure Ratio for Given Inlet Expander Pressure and Minimum Cold Side Temperature for Methanol

	Maximum Pressure Ratio					
Inlet Pressure [Bar]	**T3=40 C**	**T3=35 C**	**T3=30 C**	**T3=25 C**	**T3 = 20 C**	**T3 = 15 C**
20	57.63	73.09	93.5	120.7	157.4	207.3
15	43.22	54.81	70.13	90.54	118	155.5
10	28.82	36.54	46.75	60.36	78.69	103.6
5	14.41	18.27	23.38	30.18	39.35	51.82

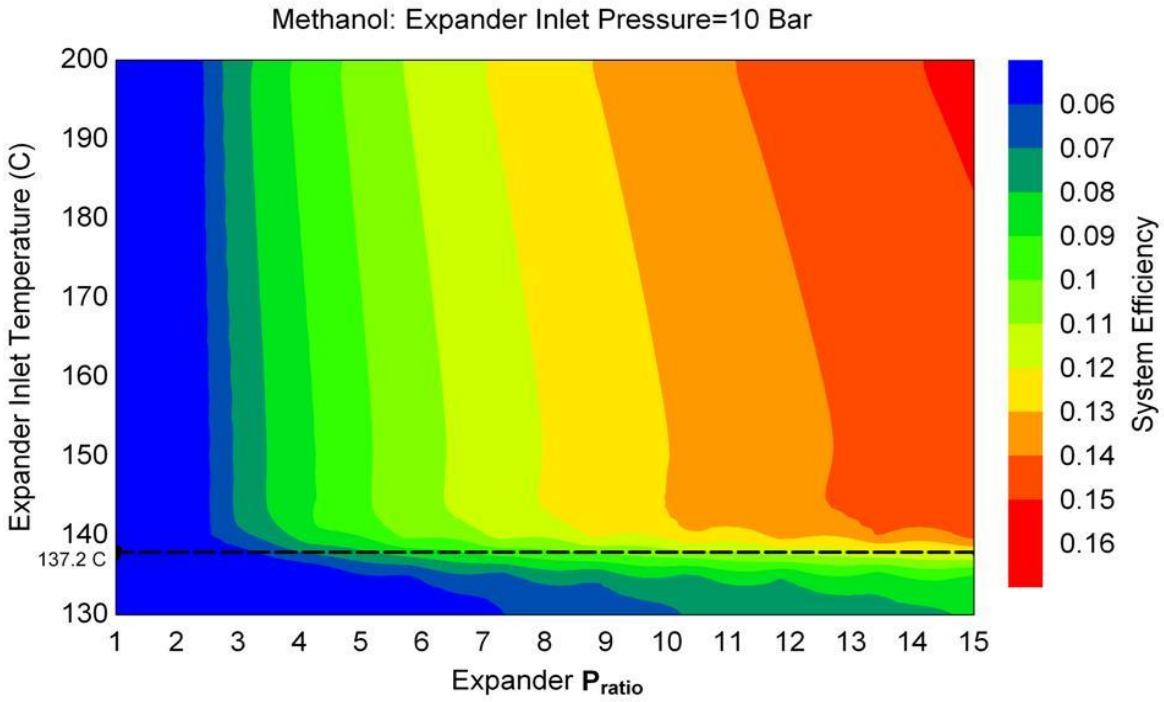

Figure 33: Methanol System Efficiency Plot for Varying Expander Inlet Temperatures and Pressure Ratios, with an Inlet Pressure of 10 Bar

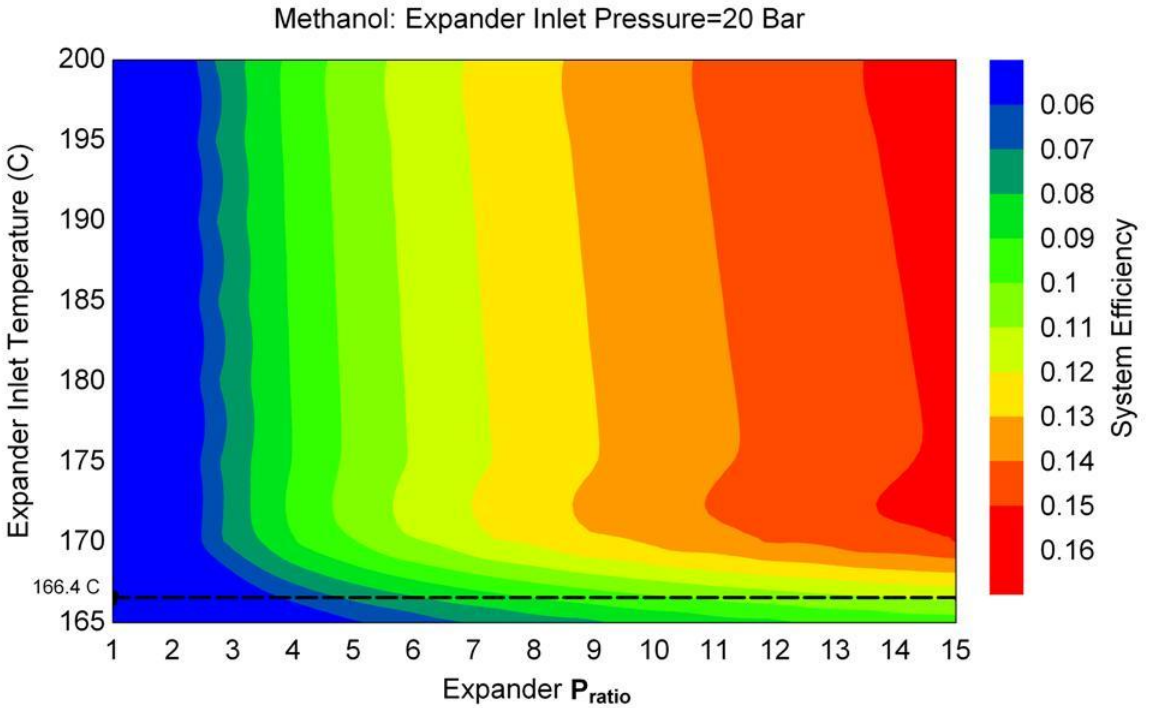

Figure 34: Methanol System Efficiency Plot for Varying Expander Inlet Temperatures and Pressure Ratios, with an Inlet Pressure of 20 Bar

3.4 Ethanol

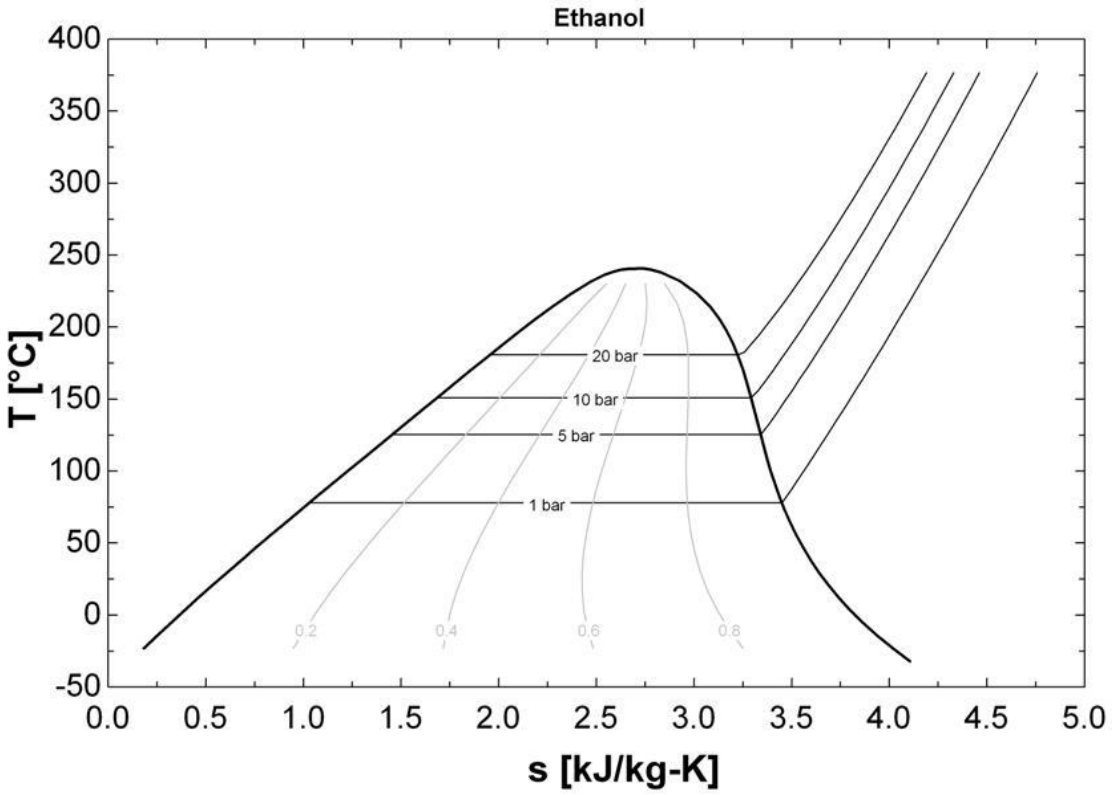

Figure 35: Ethanol Temperature-Entropy Diagram

Ethanol is an alcohol that is very similar to methanol and it shares many of the same attributes. As Figure 35 above shows, the two substances have comparable T-s diagrams. Like methanol, ethanol is created organically so there are no potential environmental concerns to deal with. Currently ethanol is being explored as a possible alternative gasoline so availability will not be a problem. The thermodynamic trends for the different system configurations coincide closely with what was observed with methanol.

When superheating the substance in a four stage Rankine cycle, the fluid behaves the same as methanol did. There is always a gain in efficiency when superheating is involved, and the higher the temperature is raised beyond the vaporization point, the more effective the system becomes. The closed loop pre-heater design for ethanol also follows the trends of methanol. Figure 36 shows that there is no added benefit of a pre-heater unless superheating is involved.

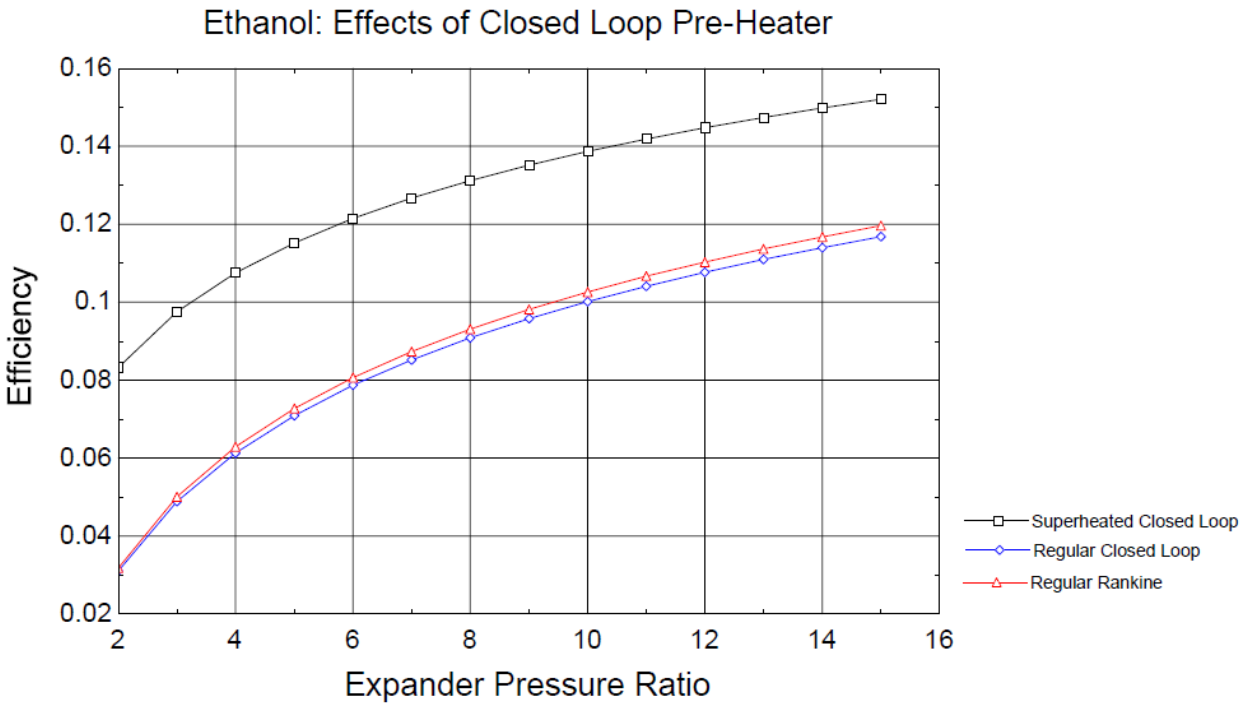

Figure 36: Effects of Closed Loop Pre-Heating with Optional Superheating for Ethanol

Due to the thermodynamic properties of ethanol, it can accommodate large expander pressure ratios as shown in Table 10. This means that no matter what the cold side temperature is limited to, the system can have a pressure ratio that is within the range of values determined by the hardware of the expander. Although ethanol is capable of large pressure ratios, compared to

Table 10: Maximum Expander Pressure Ratio for Given Inlet Expander Pressure and Minimum Cold Side Temperature of Ethanol

	Maximum Pressure Ratio					
Inlet Pressure [Bar]	**T3=40 C**	**T3=35 C**	**T3=30 C**	**T3=25 C**	**T3 = 20 C**	**T3 = 15 C**
20	111.8	145.5	191.3	254.1	341.2	463.5
15	83.83	109.1	143.5	190.6	255.9	347.6
10	55.89	72.75	95.64	127	170.6	231.7
5	27.94	36.38	47.82	63.52	85.3	115.9

the other working fluids, it needs higher temperatures to have a phase change. Figures 37 and 38 show the 3D efficiency plots for ethanol at inlet pressures of five and ten Bar respectably. The lower inlet pressures were explored due to the required input energy at higher pressures.

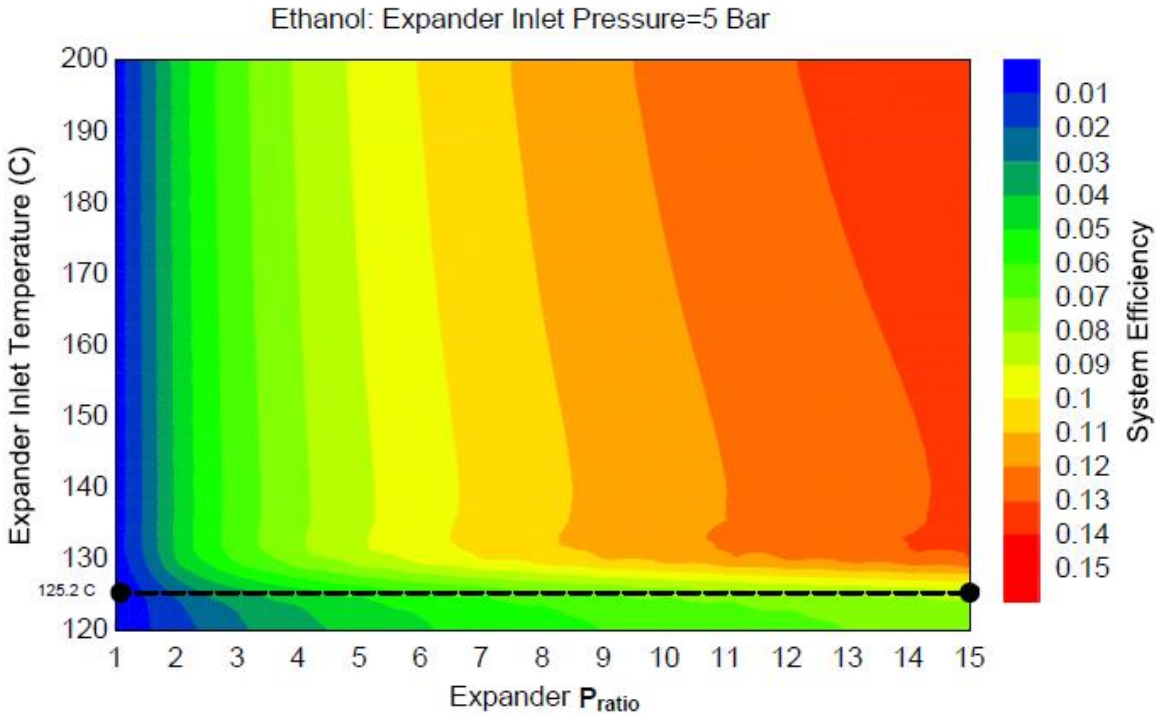

Figure 37: Methanol System Efficiency Plot for Varying Expander Inlet Temperatures and Pressure Ratios, with an Inlet Pressure of 20 Bar

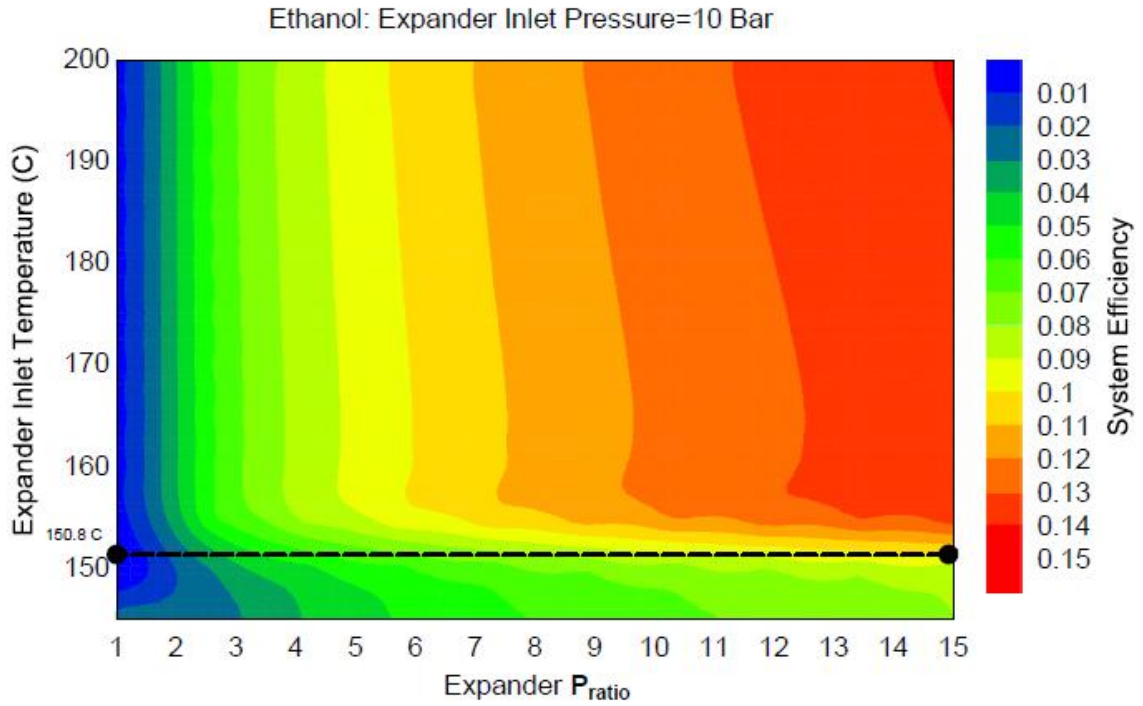

Figure 38: Methanol System Efficiency Plot for Varying Expander Inlet Temperatures and Pressure Ratios, with an Inlet Pressure of 20 Bar

Chapter 4: Conclusion and Recommendations

4.1 Summary of Different Working Fluids

Each one of the working fluids that were explored demonstrated potential. Depending on inlet conditions and selected system configuration, each substance was capable of system efficiencies that compete with current photovoltaic technology. What the hardware of the system is capable of will dictate which of the working fluids is best suited for the cycle. The selection of a substance will depend on three main constraints: the amount of energy available from the solar collectors, the pressure ratio of the expander, and the cold side temperature of the condenser.

Out of the four possible fluids, iso-butane is best suited for lower expander input temperatures. If the solar collectors can raise the temperature of the fluid to a range of 80°C to 125° C, R600a will give the best results as far as system efficiency goes. In this temperature range, iso-butane will require pressure ratios below 8 and can yield efficiencies up to 14%. An added benefit of R600a is that there is no advantage to superheating the regular Rankine cycle. So if the limiting factor in the system is the inlet temperature from the collectors, iso-butane has the advantage of being most efficient when heating just to the vaporization temperature. The drawback to using iso-butane is that its efficiency is heavily dependent on the available cold side temperature. Depending on whether the system is rejecting heat to 40° C or 15° C, the system can have an efficiency ranging from 8% up to 14% respectably. This also means that there is little to no opportunity of using iso-butane for co-generation processes.

N-pentane has very similar drawbacks to iso-butane but it requires a higher temperature input to get the same efficiencies. When compared to R600a, there is no benefit to using n-pentane if a regular four stage Rankine cycle is to be used as the system configuration. The optimization of n-pentane comes in the closed loop pre-heater design. When a per-heater is used

in combination with superheating, the system can reach an efficiency of 14.9% with an expander inlet temperature of 102.5° C and a pressure ratio of 5. If there is enough solar energy available to raise the inlet temperature to 151.7° C, an efficiency of 21.15% can be achieved with a pressure ratio of 15.

Methanol and ethanol carry many of the same advantages and disadvantages as one another. Compared to the other fluids, both ethanol and methanol require higher vaporization temperatures at similar pressures. With an inlet pressure of 10 Bar, methanol and ethanol need vaporization temperatures of 137.2° C and 150.8° C, respectably. If these temperatures can be reached, methanol can reach efficiencies in the range of 10-13% for pressure ratios of 5 to 10 and ethanol can be 9-13% efficient for pressure ranges from 6-10. Due to the greater high side temperature of the cycle, there is not a strong correlation between the system efficiencies of the two fluids and the low side condenser temperature. A major benefit of these substances is their commercial availability in today's world and compatibility with co-generation applications due to rejecting heat at higher temperatures. Both fluids see a positive effect on the efficiency when superheating of the regular Rankine cycle occurs but it is only on the order of one additional percent of efficiency for an extra 80° C of heat input. Of the two fluids, methanol would be better suited for this application.

4.2 Summary of System Configurations

The selection of system configuration will depend on hardware constraints as well as the working fluid. The regular four stage Rankine cycle is best suited for an application with an inlet temperature ranging from 80°C to 125° C with iso-butane as the working fluid. If n-pentane is chosen as the cycle substance, the closed loop pre-heater should be implemented. As for the superheating or a regular Rankine cycle, there were no scenarios where the benefits outweighed

the additional energy that was required. No matter which fluid is selected, if a closed loop pre-heater configuration is implemented, superheating should be utilized if the energy is available. When exploring the possibility of an open loop pre-heater design, it was decided that the additional 1.6% gain in efficiency was not worth the associated hardware costs. Since this thesis focused only on the efficiency of electricity generation of the system and didn't explore the effects of co-generation, the most promising configuration would be a closed loop pre-heater design.

4.3 Recommended Research

All of the research that has been documented in this paper has been strictly theoretical. The numerical analysis that has been preformed may not directly correlate with results from real world experiments. However, the calculated data does narrow down what types of configurations should be investigated in further detail. The research also brackets and quantifies a range of results to be expected for the best case scenarios. This information can be used to pinpoint areas where future research will be most beneficial.

One area where additional research could be explored is in the area of co-generation. All of the work that was done in this paper was about creating a system that could compete with photovoltaic cells in terms of electricity generation. As mentioned in the introduction, one of the advantages of solar thermal is its ability to use the energy it collects for multiple purposes. An energy and cost analysis on a typical residential house should be done to see how effectively the system can use the thermal energy it collects from the sun. It could be found that although PV panels are more efficient at creating electricity, the complete solar thermal design may save more energy and money because it can be used for electricity, heat, hot water and other applications.

The other area of continued work should be in creating a dynamic model of the system. All of the research that has been done so far has only looked at a system with both static solar input and constant electrical loads. This is just not representative of a real world scenario where the heat input will vary due to the sun and the electrical load will vary due to user needs. The work done for this thesis is a great launching point for creating the dynamic model. Using tables generated in EES that give system efficiency and net work as a function of static inputs, like expander inlet temperature or energy entering the system, trend lines and equations of the data can be created. With these functions, software such as Simulink can be used to explore time varying inputs and the possibility of a control system to maximize overall efficiency. Another undergraduate honors student, Nicholas Warner, will be exploring this avenue for his thesis.

The idea of residential solar thermal electricity generation is still in its infancy, and there is still a lot of research to be done, but the concept seems very promising. The sun is so powerful and gives off so much energy; it is truly difficult to comprehend the magnitude of it. While I am glad that research is being done to try and capture its energy in a clean and sustainable manner, I do however fear the concept of trying to profit off our planet's most abundant and beautiful natural resource. Sunlight is not something that should be bought or sold; it is a gift that should be common to all.

References

[1] Akella, A., R. Saini, and M. Sharma. "Social, Economical and Environmental Impacts of Renewable Energy Systems." *Renewable Energy* 34.2 (2009): 390-96. Print.

[2] Schilling, Melissa A., and Melissa Esmundo. "Technology S-curves in Renewable Energy Alternatives: Analysis and Implications for Industry and Government." *Energy Policy* 37.5 (2009): 1767-781. Print.

[3] Varun, Ravi Prakash, and Inder Krishnan Bhat. "Energy, Economics and Environmental Impacts of Renewable Energy Systems." *Renewable and Sustainable Energy Reviews* 13.9 (2009): 2716-721. Print.

[4] Headings, Leon (1999) *Design and Analysis of an Automotive Thermal Energy Recovery System*. Undergraduate Honors Thesis. The Ohio State University

[5] Nguyen, V. "Development of a Prototype Low-temperature Rankine Cycle Electricity Generation System." *Applied Thermal Engineering* 21.2 (2001): 169-81. Print.

[6] Schuster, A., S. Karellas, E. Kakaras, and H. Spliethoff. "Energetic and Economic Investigation of Organic Rankine Cycle Applications." *Applied Thermal Engineering* 29.8-9 (2009): 1809-817. Print.

[7] Dai, Y., J. Wang, and L. Gao. "Parametric Optimization and Comparative Study of Organic Rankine Cycle (ORC) for Low Grade Waste Heat Recovery." *Energy Conversion and Management* 50.3 (2009): 576-82. Print.

[8] Garciarodriguez, L., and J. Blancogalvez. "Solar-heated Rankine Cycles for Water and Electricity Production: POWERSOL Project." *Desalination* 212.1-3 (2007): 311-18. Print

[9] Husband, W. W., and A. Beyene. "Low-grade Heat-driven Rankine Cycle, a Feasibility Study." *International Journal of Energy Research* 32.15 (2008): 1373-382. Print.

[10] Moran, Michael J., and Howard N. Shapiro. *Fundamentals of Engineering Thermodynamics*. Hoboken, N.J. : Chichester: Wiley ; John Wiley, 2008. Print.

[11] Tchanche, Bertrand Fankam, George Papadakis, Gregory Lambrinos, and Antonios Frangoudakis. "Fluid Selection for a Low-temperature Solar Organic Rankine Cycle." *Applied Thermal Engineering* 29.11-12 (2009): 2468-476. Print.